Equation-of-state constraints from FOPI and ASY-EOS flow measurements

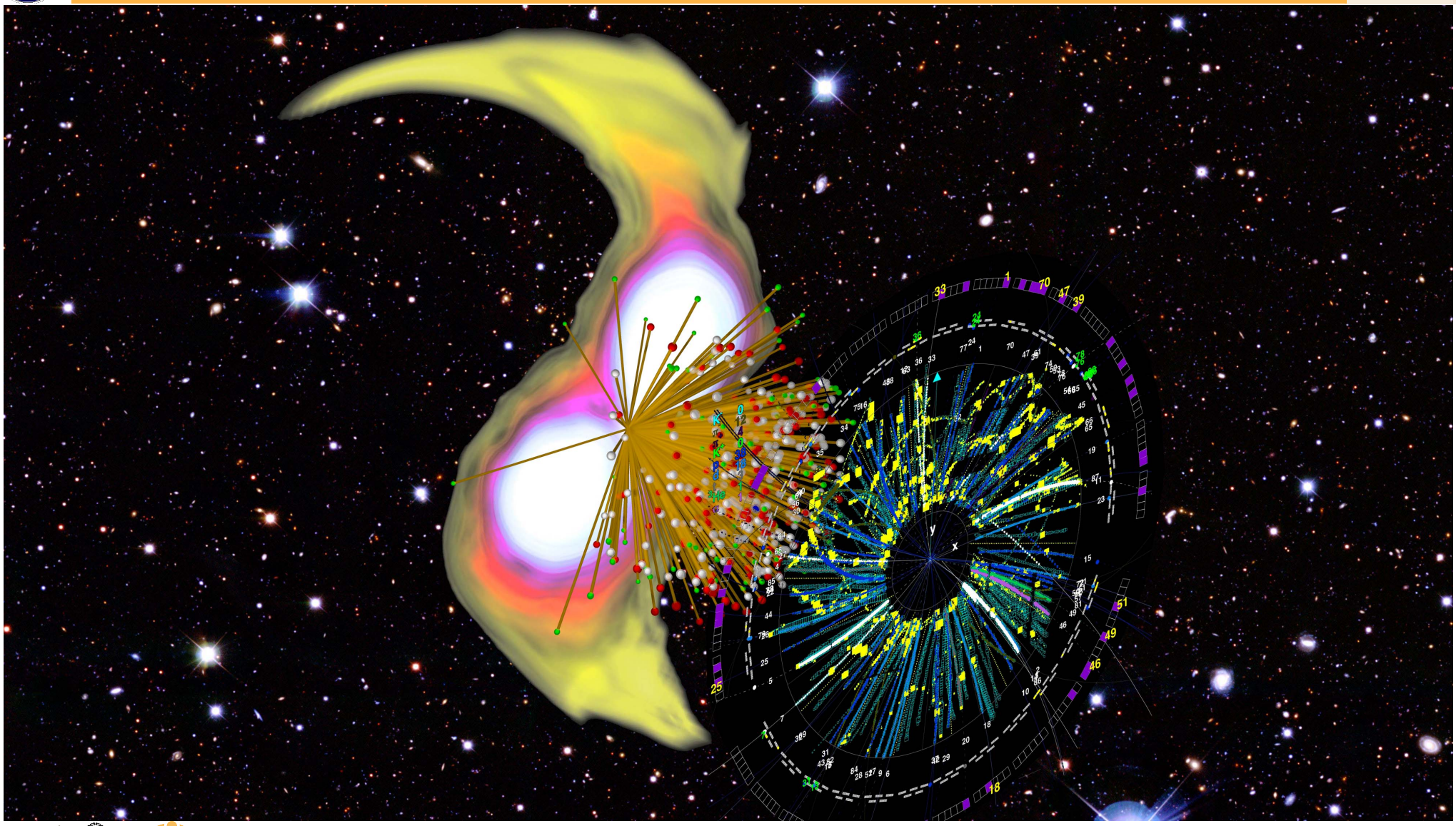

Equation-of-state constraints from FOPI and ASY-EOS flow measurements

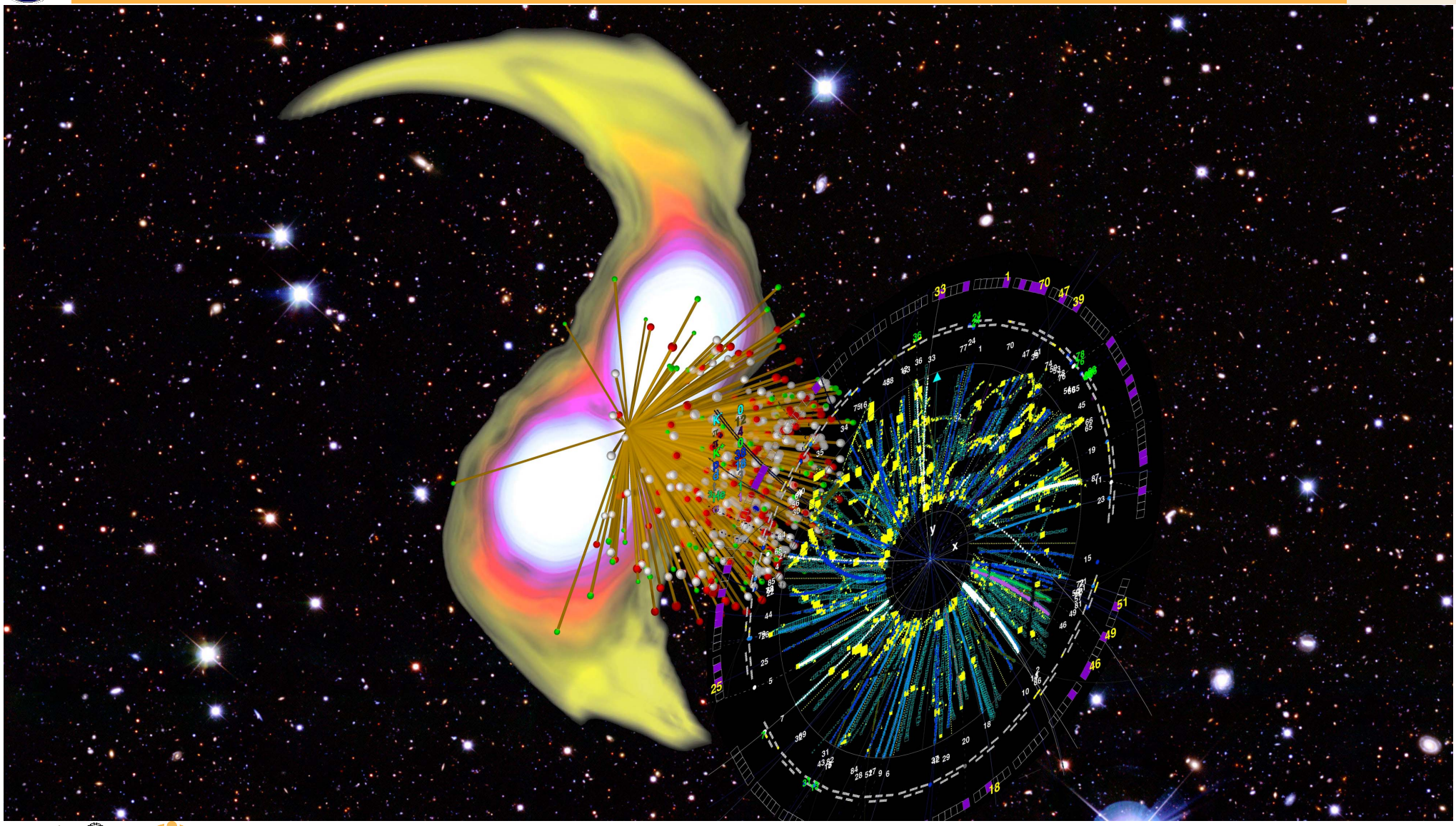

Micro- & macroscopic collisions

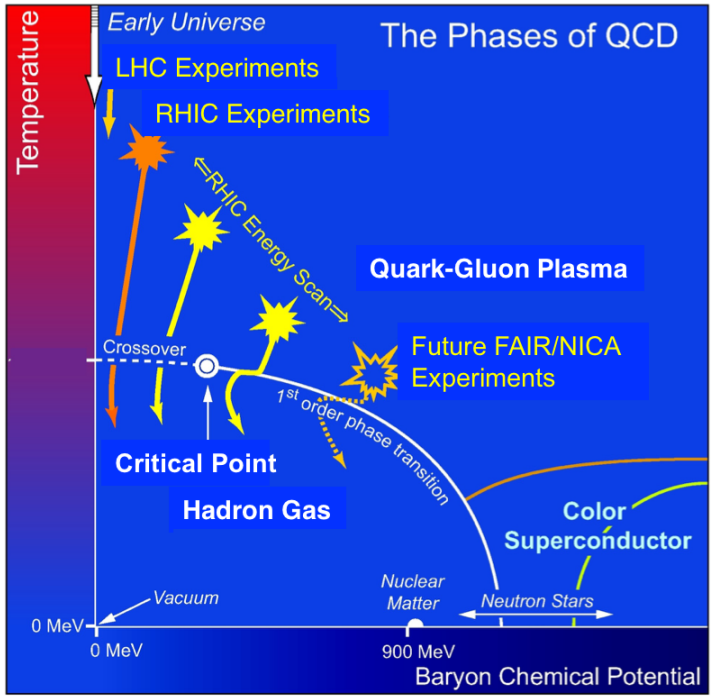

[STAR], Studying the Phase Diagram of QCD Matter at RHIC, STAR Note 598 (2014)

Micro- & macroscopic collisions

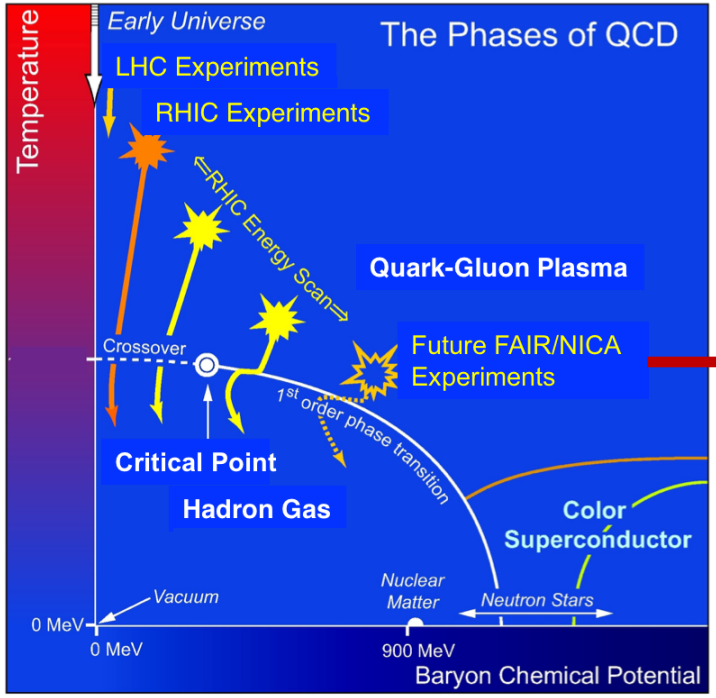

[STAR], Studying the Phase Diagram of QCD Matter at RHIC, STAR Note 598 (2014)

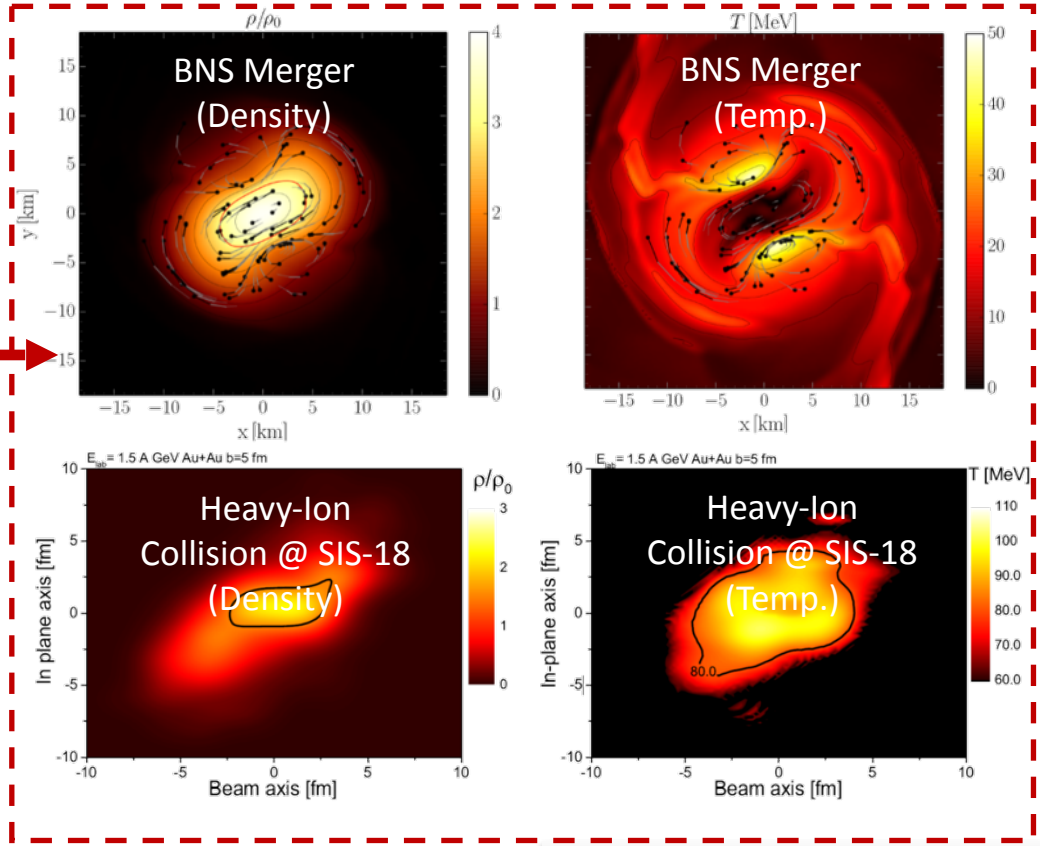

Temperature and density created in the fireball in HIC's at intermediate energies ($E_{inc} \approx 0.1 - 10AGeV$) mimic the density and temperature conditions created in binary neutron star mergers

M. Hanauske et al., 2017 J. Phys.: Conf. Ser. 878 012031

Micro- & macroscopic collisions

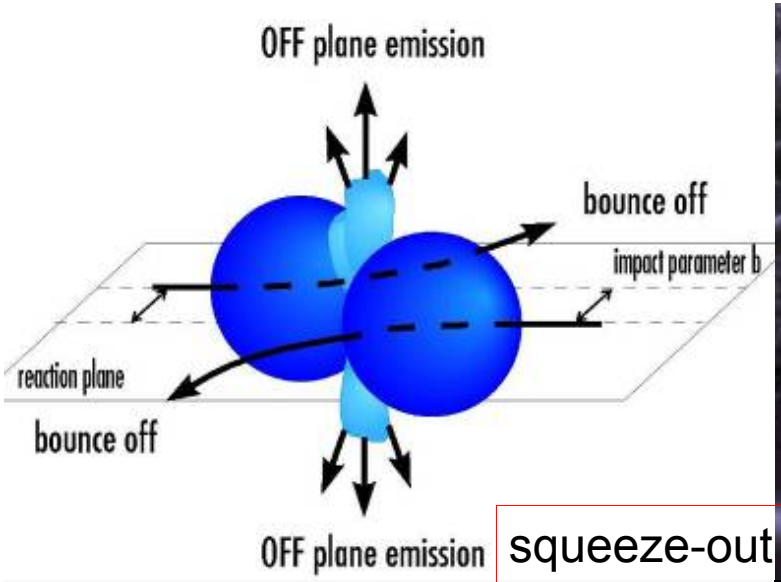

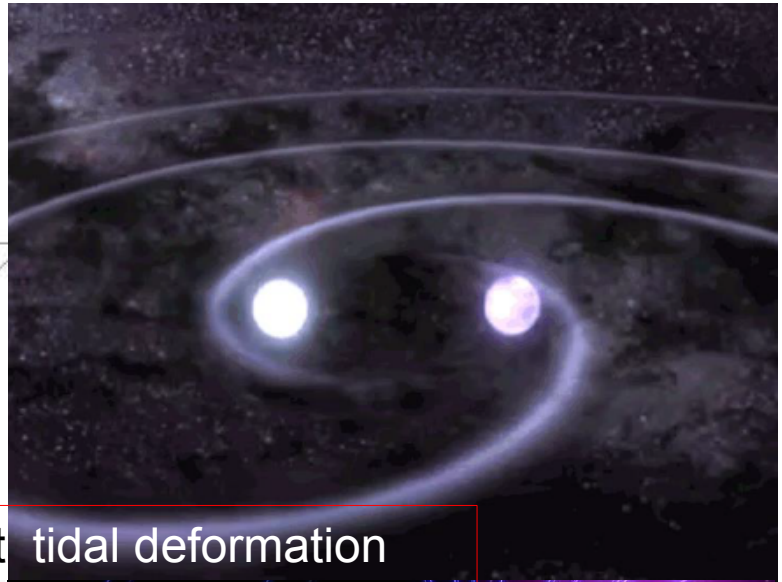

squeeze-out tidal deformation
neutron skin neutron star radius

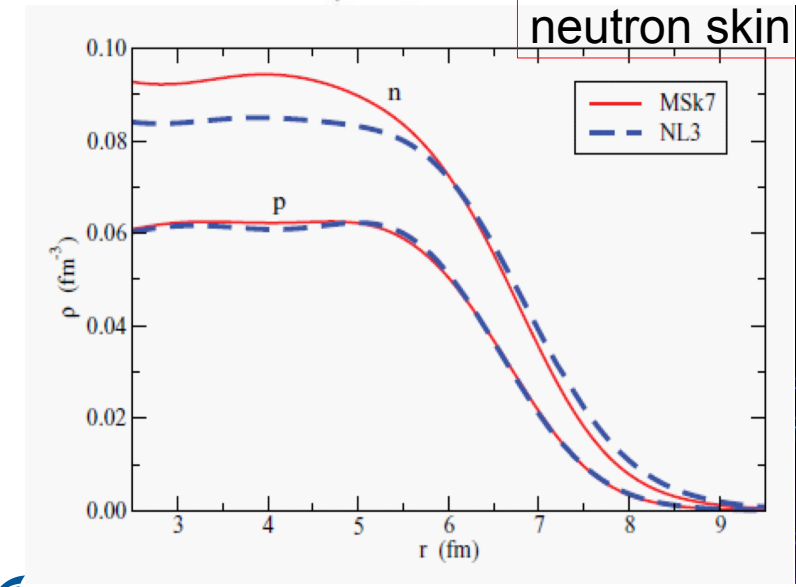

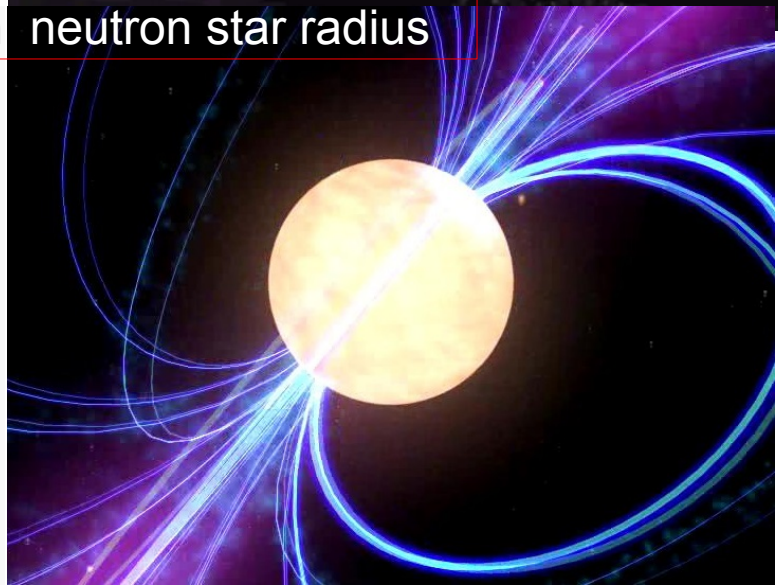

The nuclear EoS from experiments and astronomical observations

Tsang+, Nature Astronomy (2024)

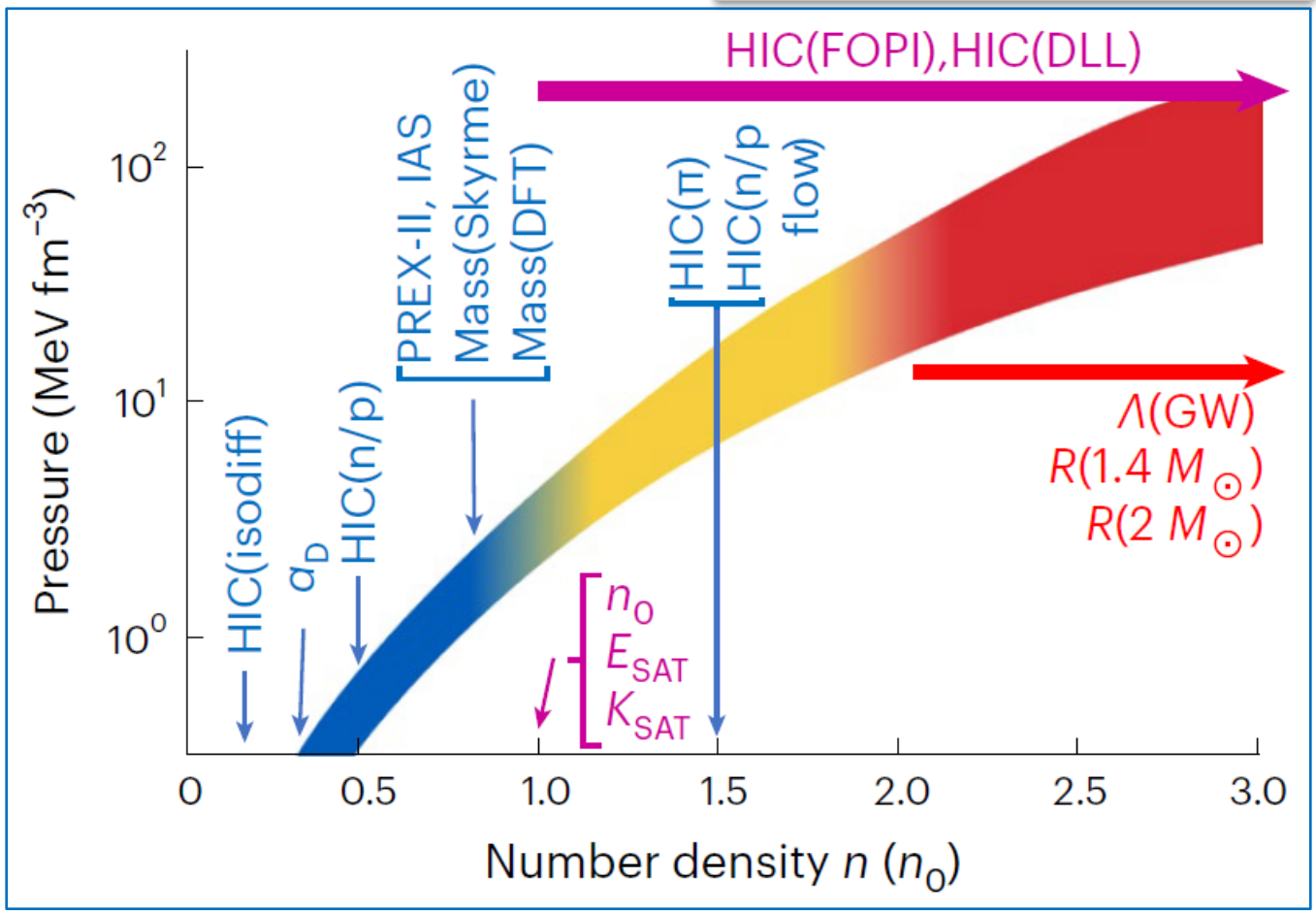

DLL: Danielewicz, Lacey, Lynch, Science - DFT: Density Functional Theory

The equation-of-state of nuclear matter

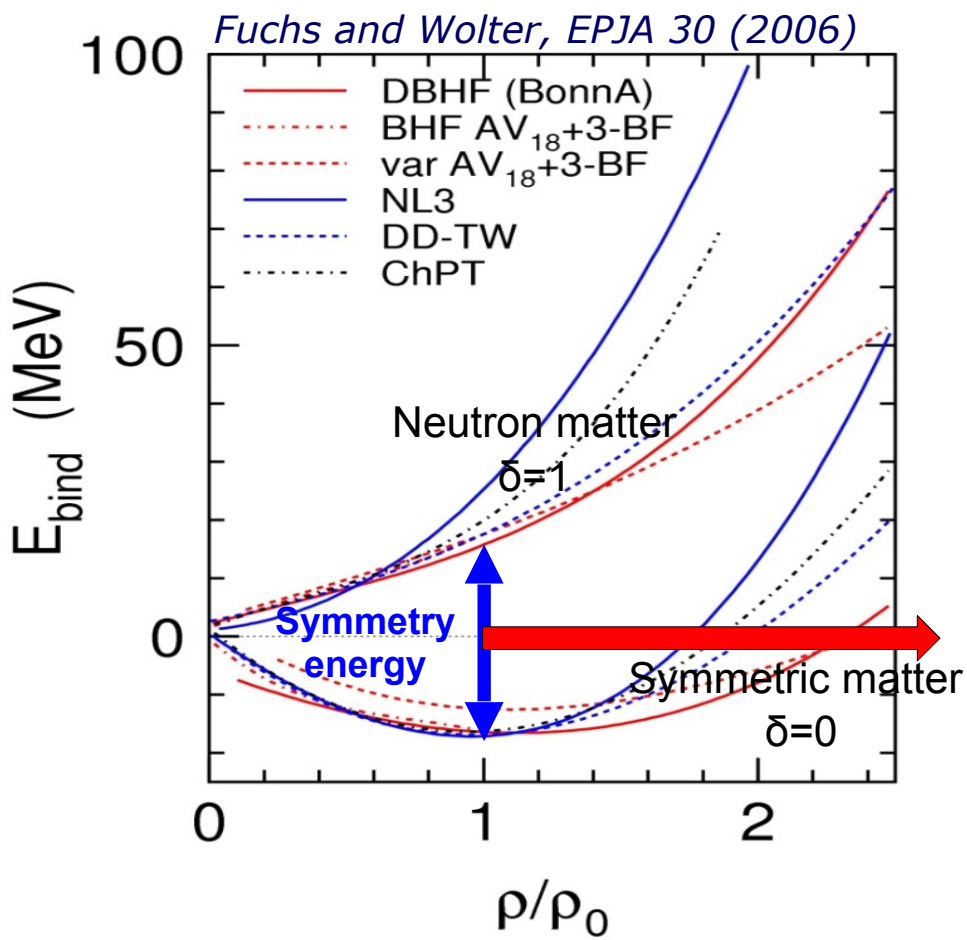

EOS in thermodynamics pressure P(ρ,T)

$$P = \rho^2 \left.\frac{\partial\, E/A}{\partial \rho}\right|_{T=const}$$

Nuclear physics EOS

$$\frac{E}{A} = \left. E/A(\rho)\right|_{T=0}$$

Nuclear incompressibility K

$$\mathrm{K} = 9\,\rho^2 \left.\frac{\partial^2\, E/A}{\partial^2 \rho}\right|_{\rho=\rho_0}$$

Asymmetry parameter $\delta = \dfrac{\rho_n - \rho_p}{\rho_n + \rho_p}$

Symmetry energy E_{sym}

$$E(\rho,\ \delta) = E_{SNM}(\rho, \delta = 0) + \delta^2 E_{sym}(\rho) + O(\delta^4)$$

mit

$$E_{sym} = E_{sym,0} + \frac{L}{3}\left(\frac{\rho - \rho_0}{\rho_0}\right) + \frac{K_{sym}}{18}\left(\frac{\rho - \rho_0}{\rho_0}\right)^2 + \ldots$$

Slope $L = 3\rho_0 \dfrac{\partial E_{sym}}{\partial \rho}$

Pressure vs density for symmetric nuclear matter

Extended Data Fig. 5 Huth et al., Nature 606 (2022)

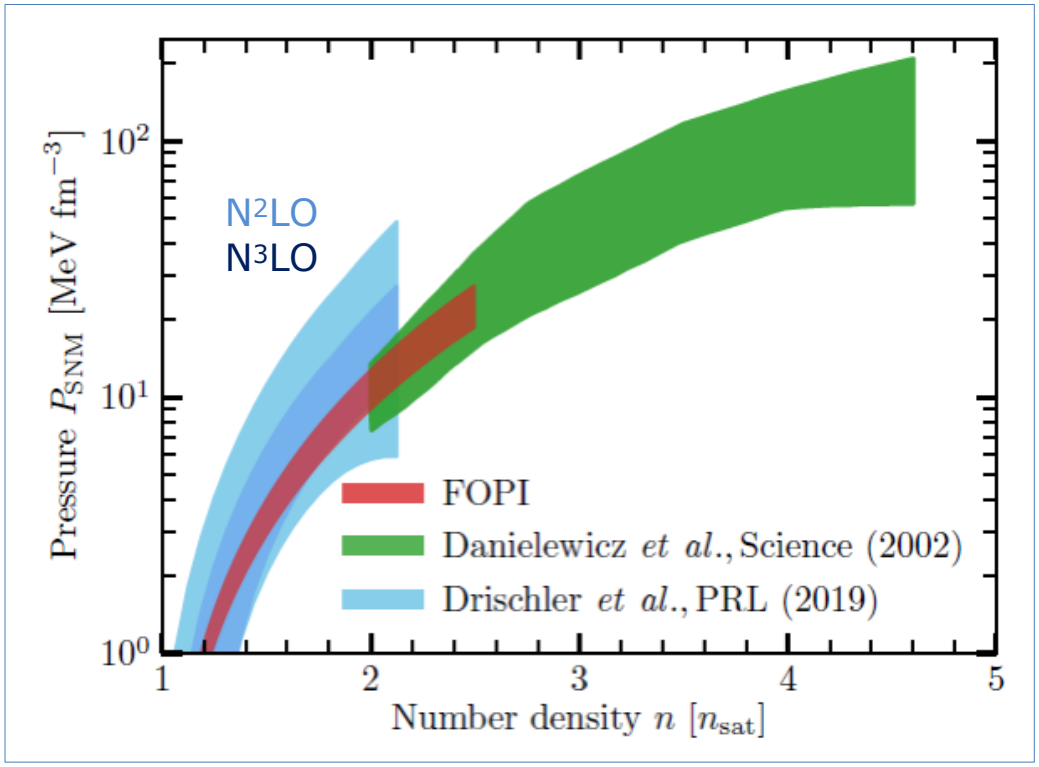

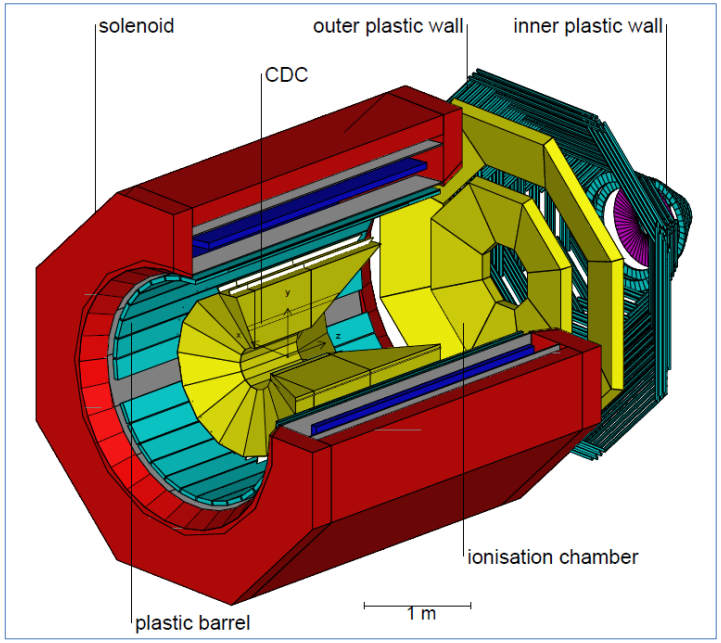

Measurements of FOPI

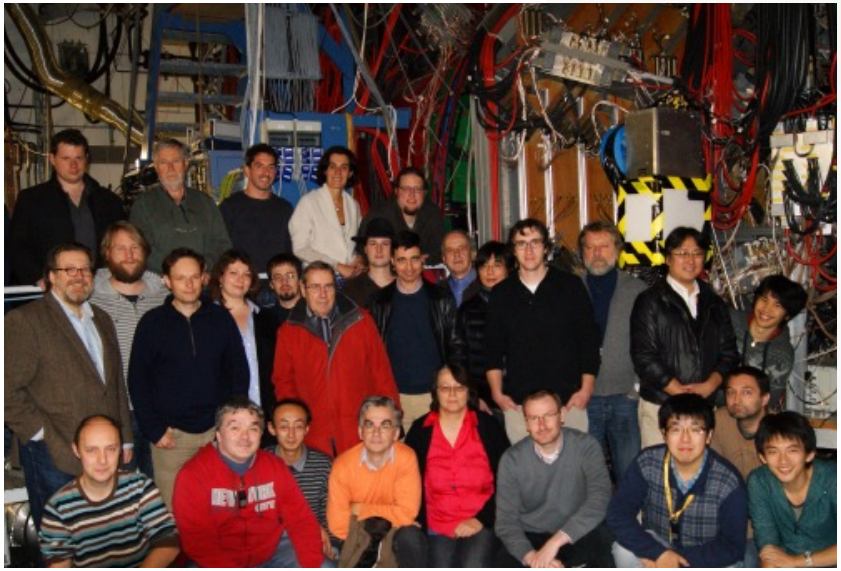

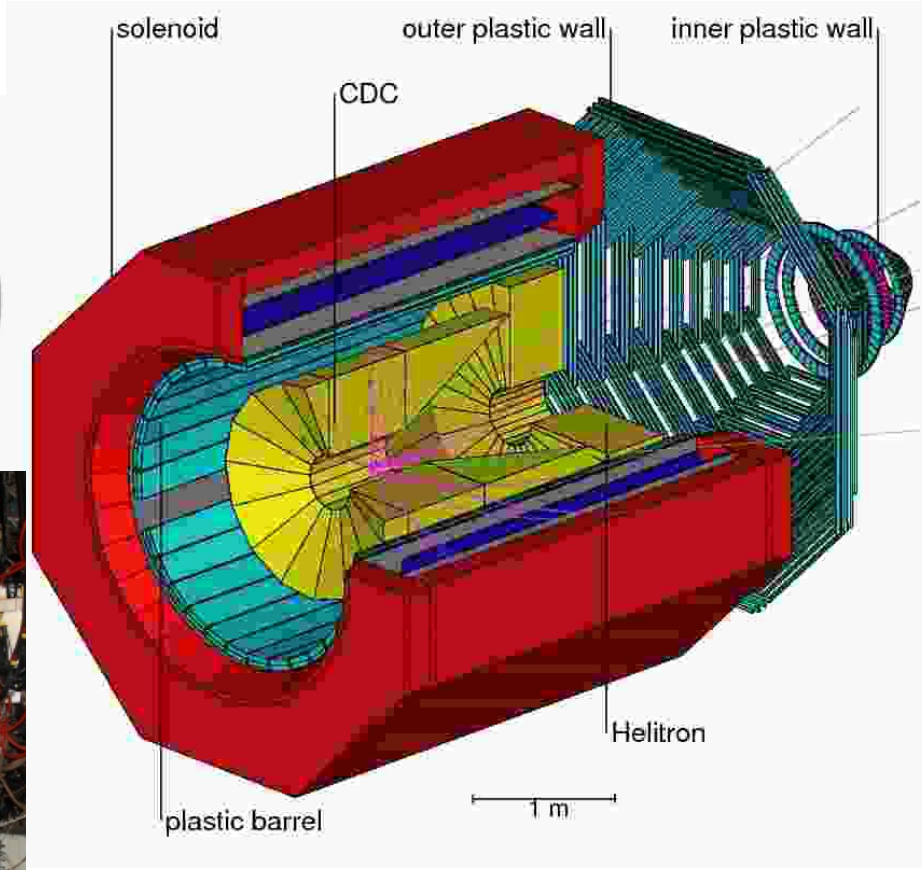

41

Measurements of FOPI

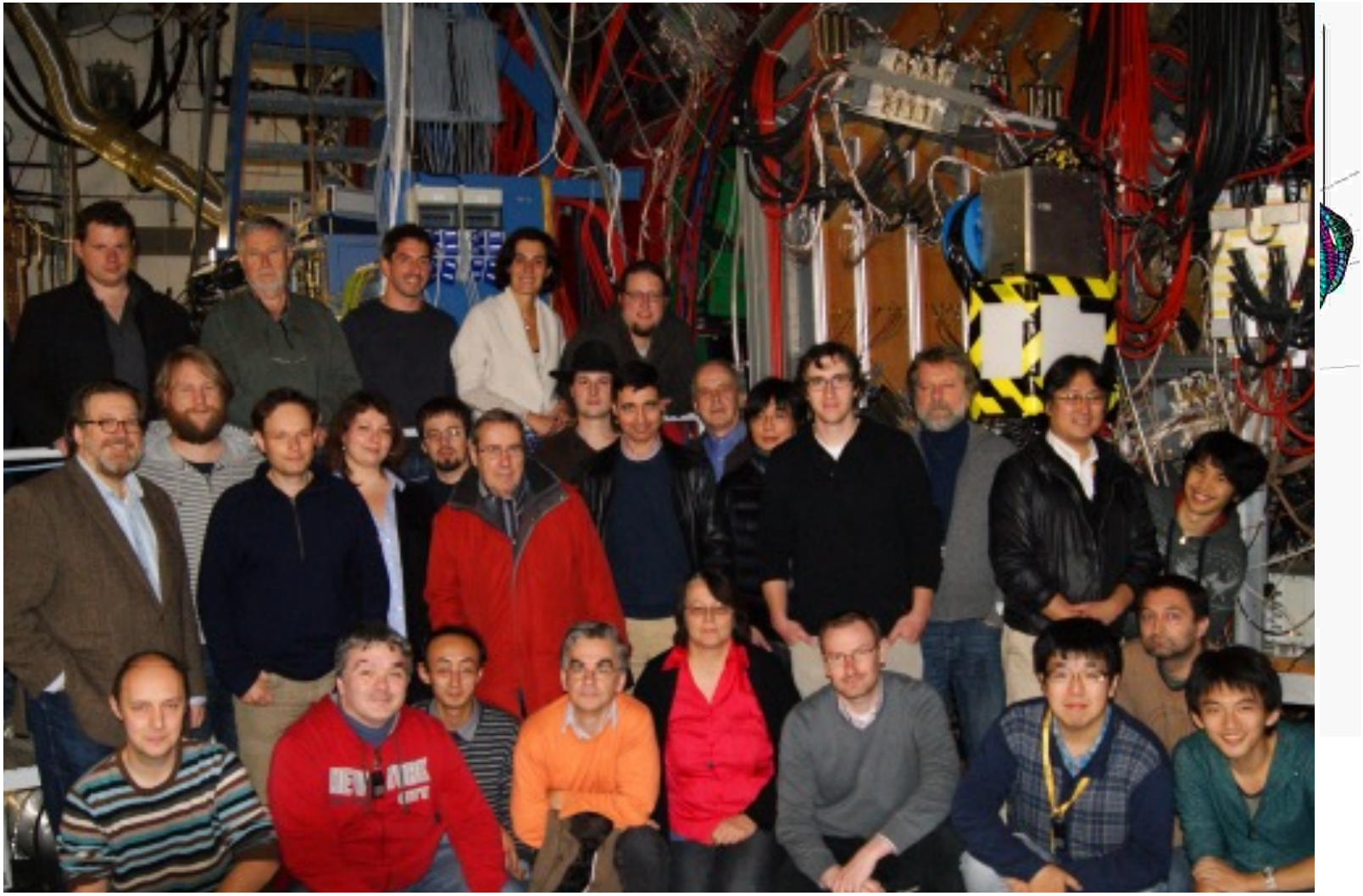

Elliptic flow method: FOPI and the incompressibility K_0

Elliptic flows of particles out of the participant region (« fireball »)

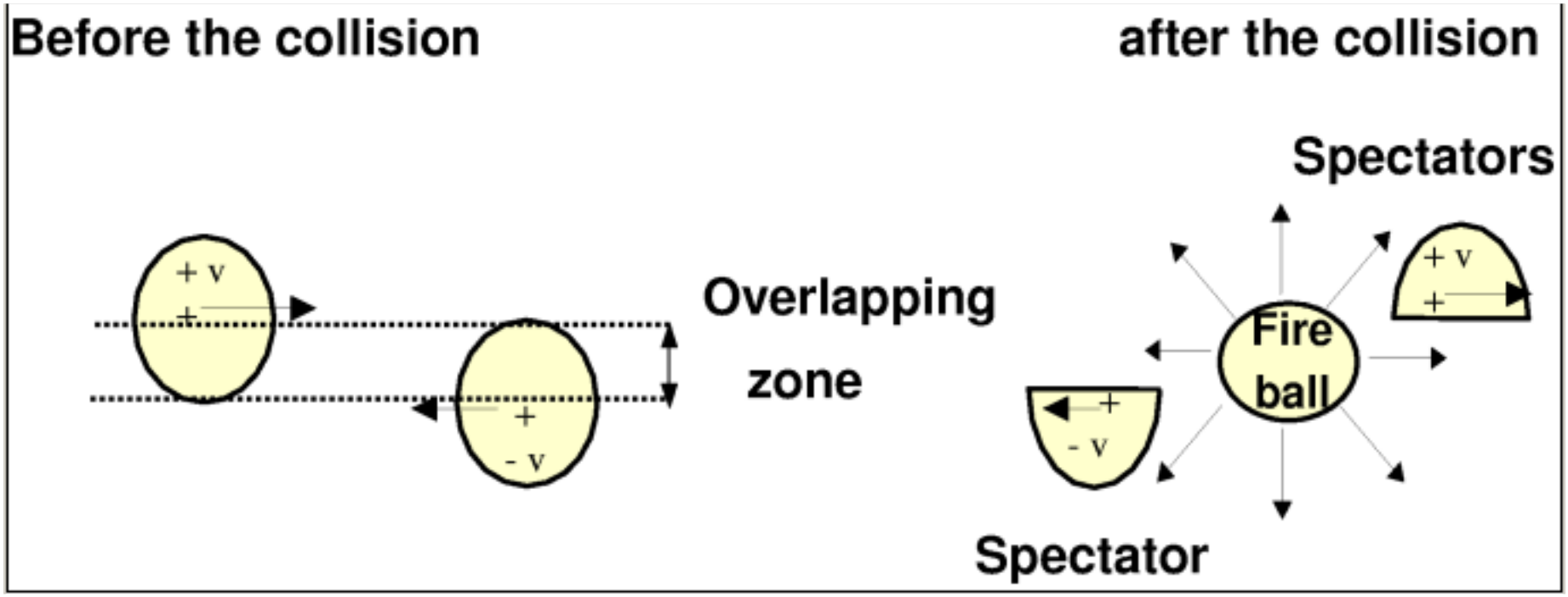

Elliptic flow method: FOPI and the incompressibility K_0

Elliptic flows of particles out of the participant region (« fireball »)

Flows at high density in heavy-ion collisions

$$\frac{dN}{d(\phi-\phi_R)}(y,p_t)=\frac{N_0}{2\pi}\left(1+2\sum_{n\geq 1}v_n\cos n(\phi-\phi_R)\right)$$

Y = rapidity

p_t = transverse momentum

Φ_R = reaction plane azimuthal angle

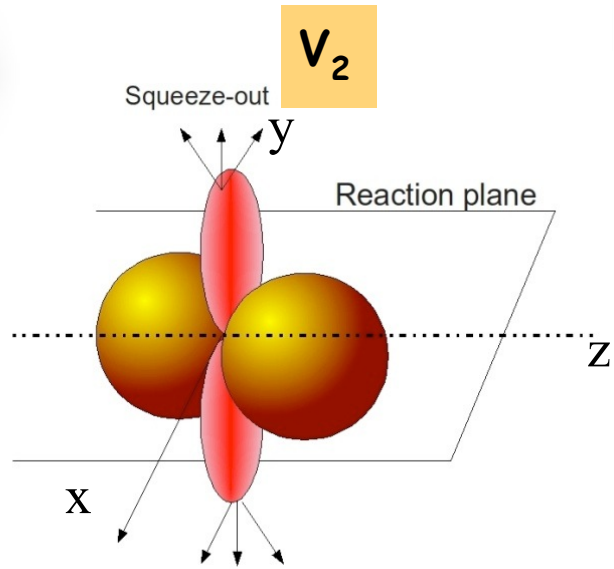

V_1 = 'side/directed flow', $\cos(\Phi-\Phi_R)$ mode

$$V_2(y,p_t)=\left\langle\frac{p_x^2-p_y^2}{p_t^2}\right\rangle$$

'Elliptic flow': $\cos(2(\Phi-\Phi_R))$ mode, competition between 'in-plane' ($V_2>0$) and 'out-of-plane' ejection ($V_2<0$).

Elliptic flow method: FOPI and the incompressibility K_0

Elliptic flow

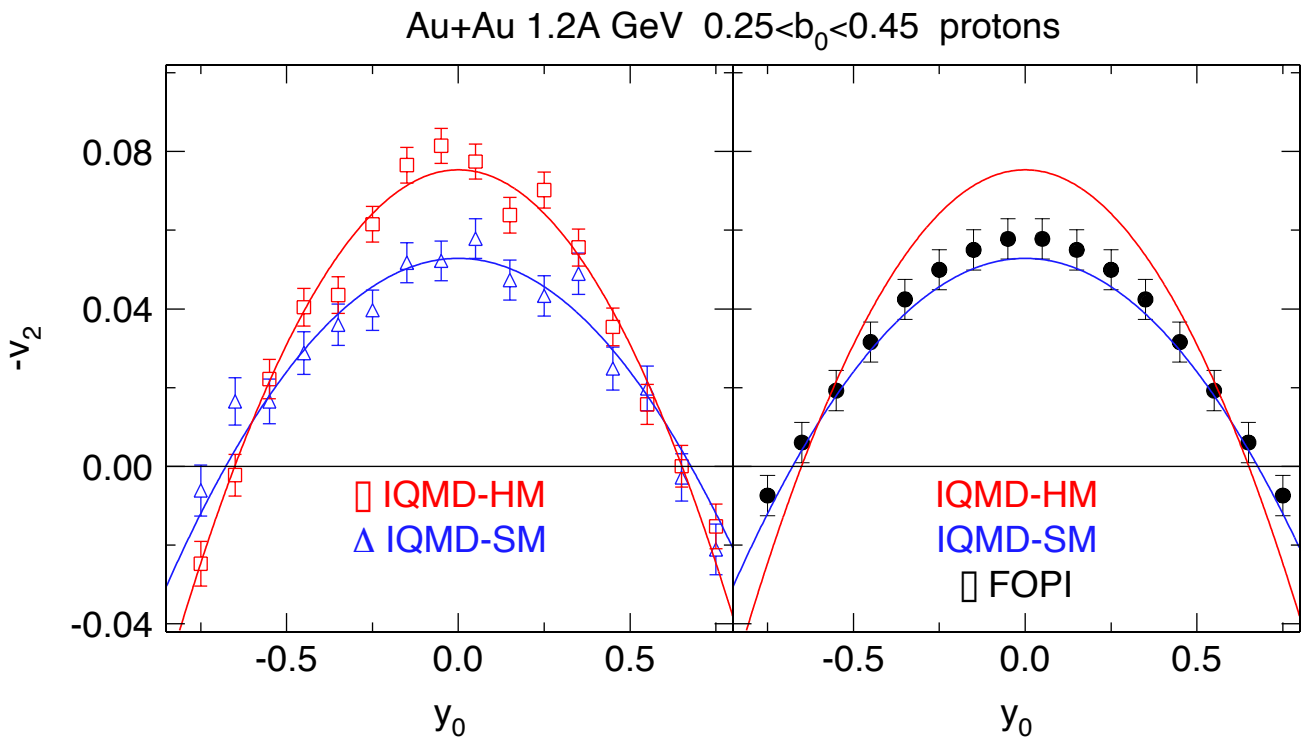

K_0 =
380 MeV ('stiff')
200 MeV ('soft')

A. Le Fèvre et al., NPA 945 (2016) 112–133

Elliptic flow method: FOPI and the incompressibility K_0

Elliptic flow

Complete shape of $v_2(y_0)$:
a new observable:
$v_{2n} = |v_{20}| + |v_{22}|$,
from fit
$v_2(y_0) = v_{20} + v_{22} \cdot y_0^2$

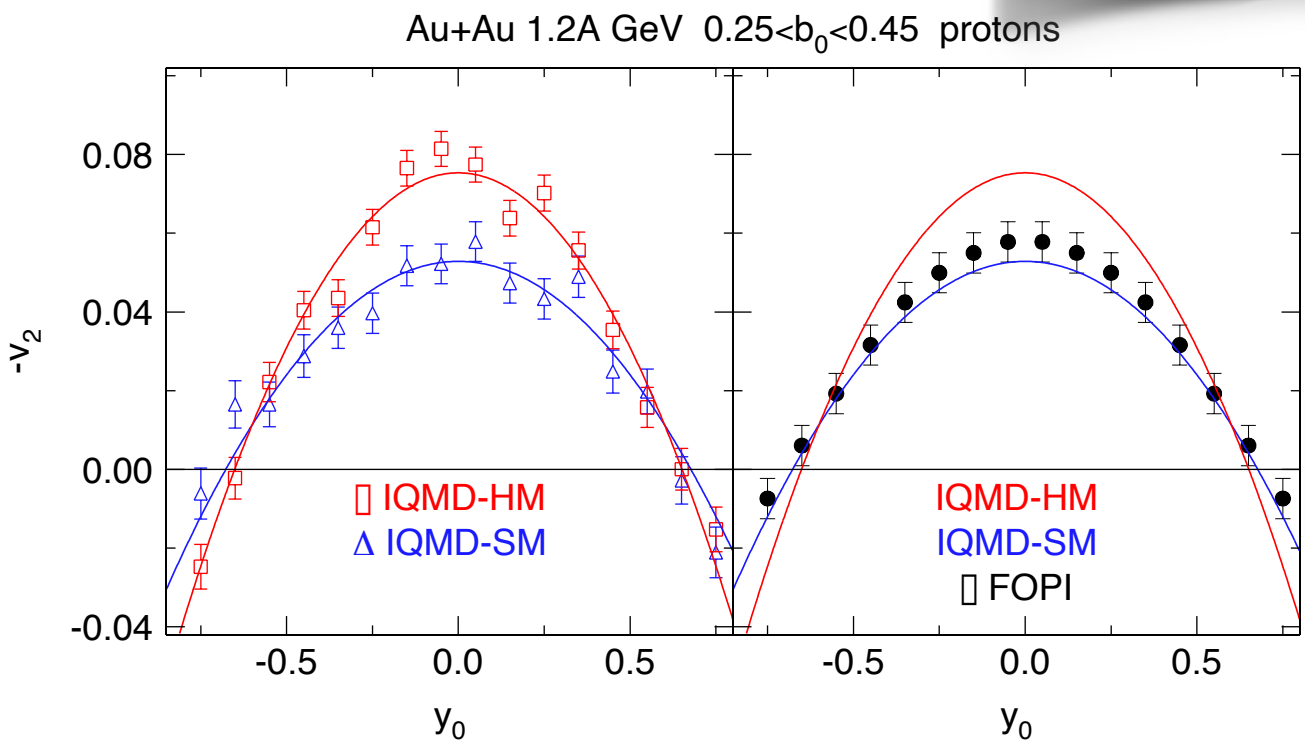

K_0 =
380 MeV ('stiff')
200 MeV ('soft')

A. Le Fèvre et al., NPA 945 (2016) 112–133

Elliptic flow method: FOPI and the incompressibility K_0

➜ $v_{2n}(E_{beam})$ varies by a factor ≈1.6, >> measured uncertainty (≈1.1)
➜ clearly favors a 'soft' EOS.

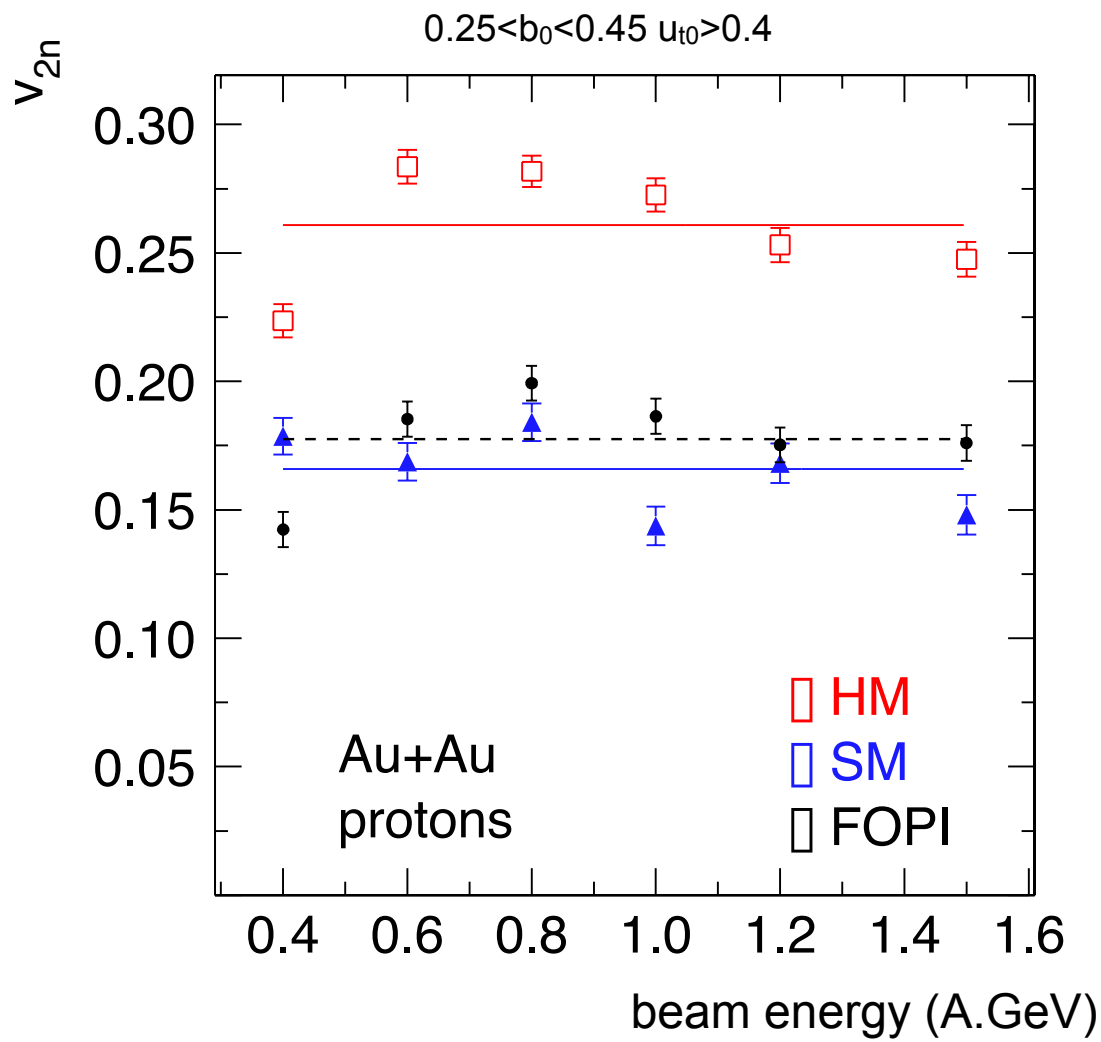

A. Le Fèvre et al., NPA 945 (2016) 112–133

Elliptic flow method: FOPI and the incompressibility K_0

➜ $v_{2n}(E_{beam})$ varies by a factor ≈1.6, >> measured uncertainty (≈1.1)
➜ clearly favors a 'soft' EOS.

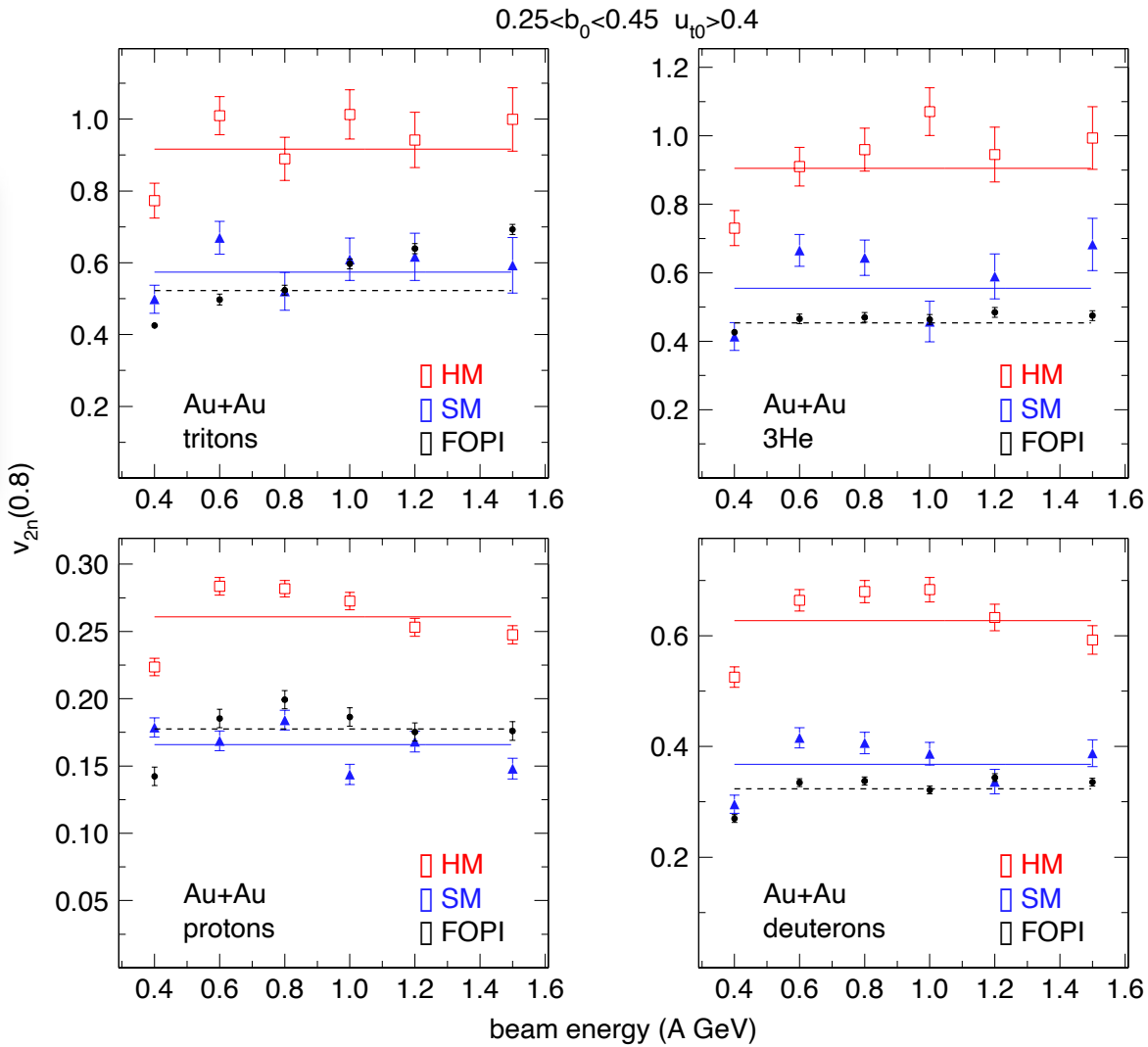

A. Le Fèvre et al., NPA 945 (2016) 112–133

Historical evidences of the need for momentum dependent interaction

- Directed flow (v_1) in semi-central collisions:
  A. Andronic et al. (FOPI Collaboration), PRC 67, 034907 (2003)

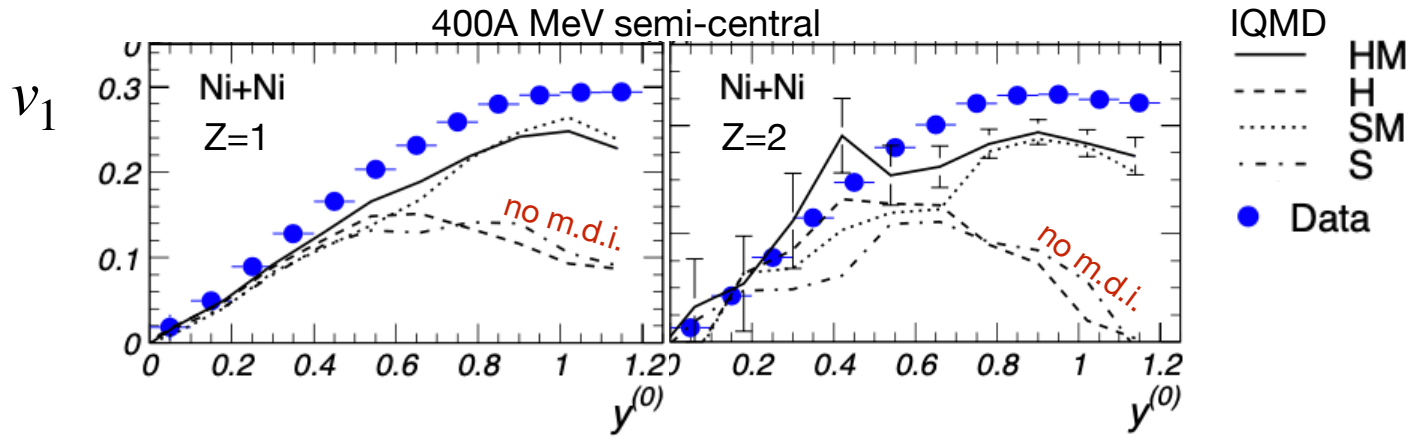

- Subthreshold kaon data (KaoS) clearly advocate a **soft** EoS :
  « Hadronic Matter is Soft », Ch. Hartnack, H. Oeschler and J. Aichelin, PRL 96, 012302 (2006)

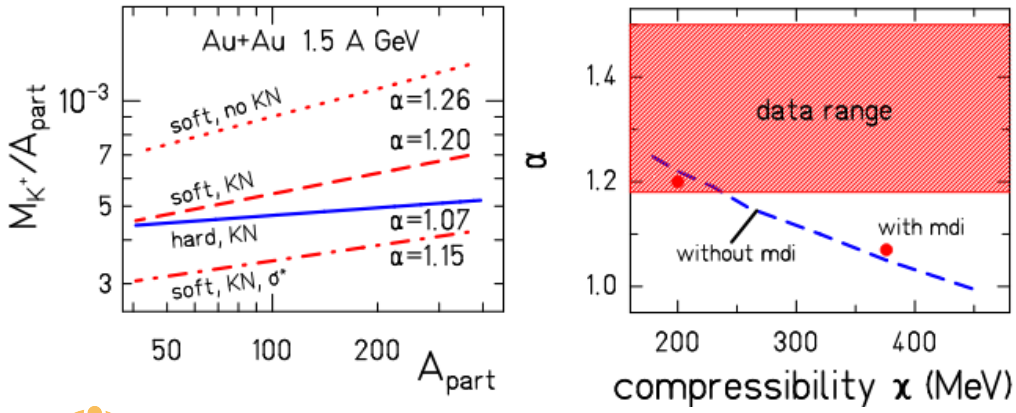

- Elliptic flow data can be explained by a **soft** EoS <u>only if m.d.i. is included</u>

Recent FOPI flow data analysis

Tarasovicova et al., Eur. Phys. J. A 60, 232 (2024)

SMASH:

- Soft momentum-dependent interaction (SP) favoured.
- At the highest inc. energies, harder EoS required
- Weakness of this analysis : restricted to Z=1

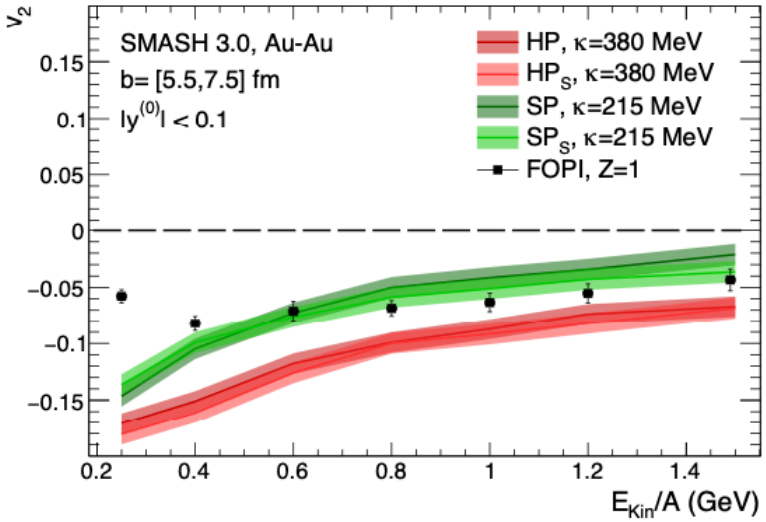

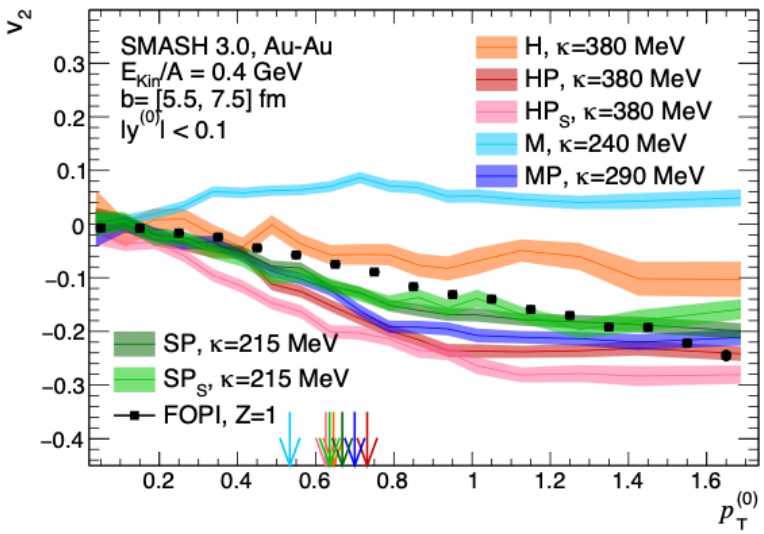

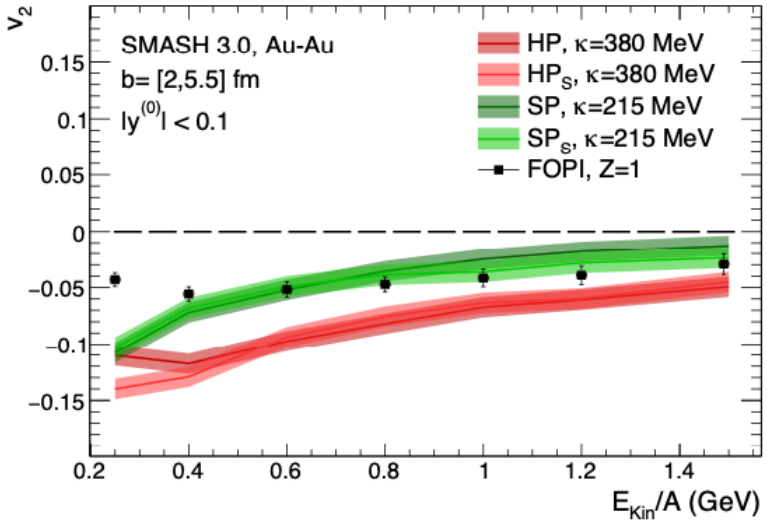

Recent FOPI flow data analysis

M.D. Cozma, Phys. Rev. C 110 (2024) 0649111

dcQMD:

- A comprehensive data analysis
- Optimisation on various parameters, assumptions, such as to narrow down constraints

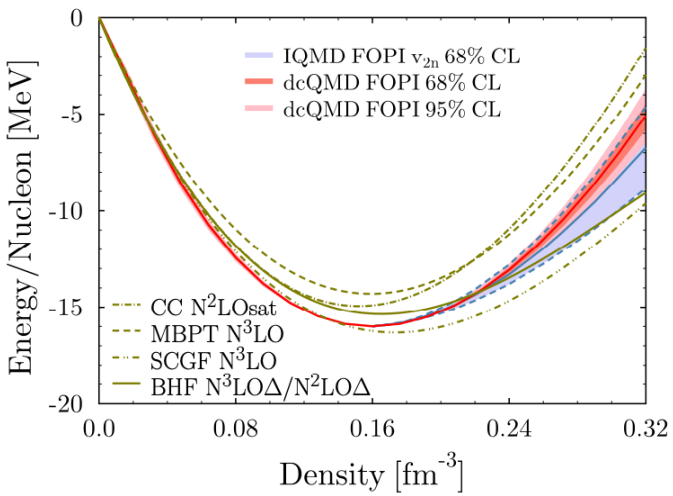

$dcQMD -> K_0 = 230^{+9}_{-11}\ MeV$

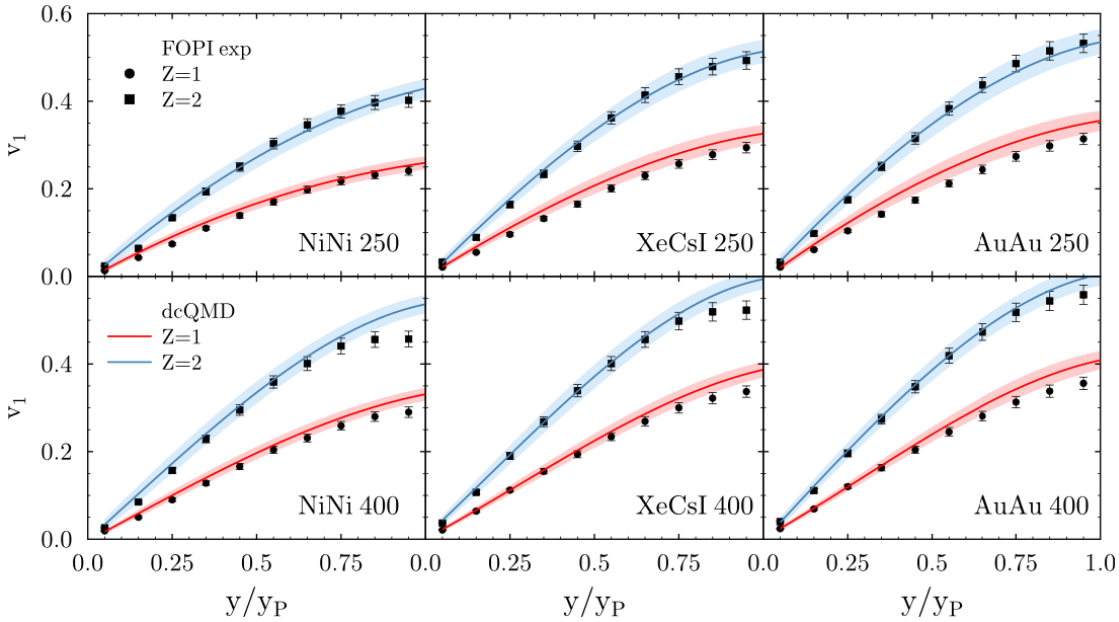

Cf. M.D. Cozma's talk on Thursday

Origin of elliptic flow: collisions versus mean field

An observable to quantify their respective contribution to it: transverse momentum modification induced projected on the direction of the final momentum:

$$\langle \Delta P_t^o(t) \rangle = \langle \boldsymbol{\Delta P_t}(t) \cdot \frac{\boldsymbol{p}_{final}}{|\boldsymbol{p}_{final}|} \rangle$$

IQMD, Au+Au, mid-central
0.6 A.GeV, mid-rapidity, u_{t0}>0.4

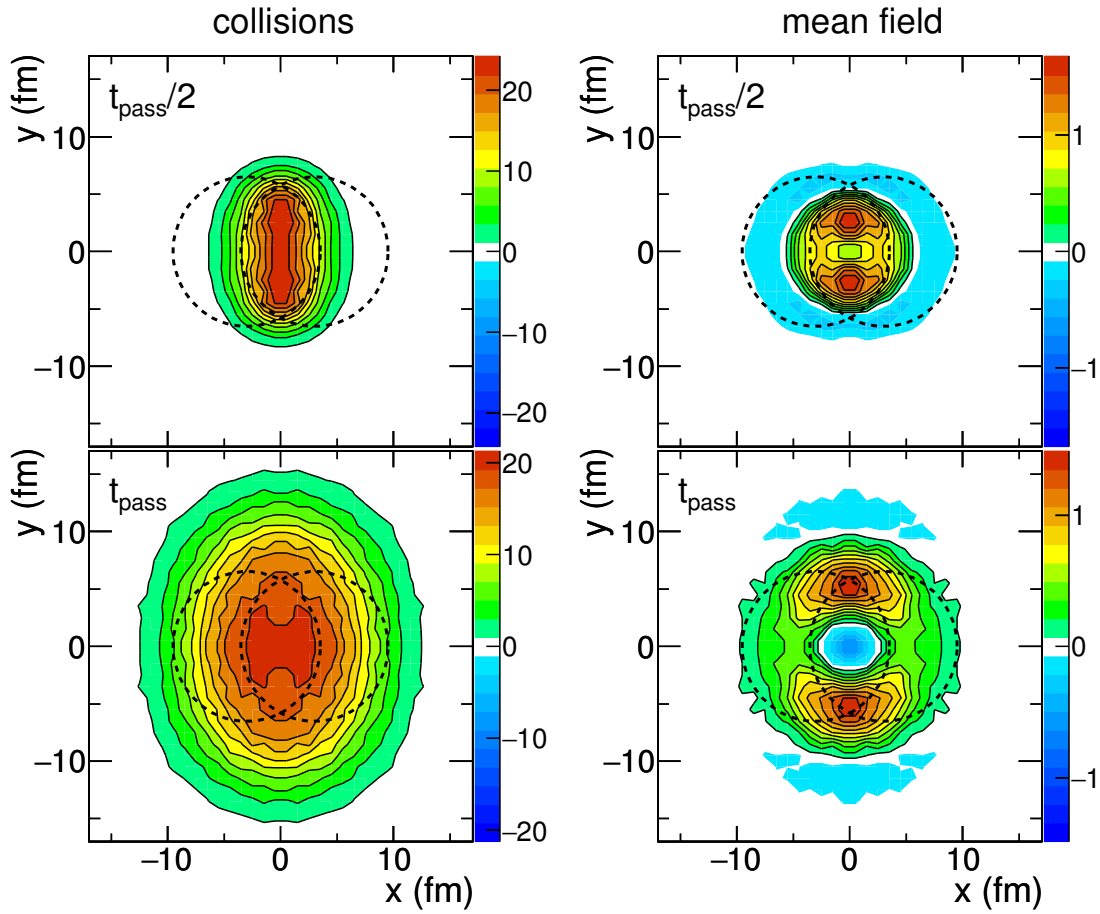

A. Le Fèvre et al., PRC98 (2016) 034901

Origin of elliptic flow: collisions versus mean field

An observable to quantify their respective contribution to it: transverse momentum modification induced projected on the direction of the final momentum:

$$\langle \Delta P_t^o(t) \rangle = \langle \boldsymbol{\Delta P_t}(t) \cdot \frac{\boldsymbol{p}_{final}}{|\boldsymbol{p}_{final}|} \rangle$$

From collisions: about an order of magnitude larger than from mean field, set fast in the overlap zone ⇨ this zone of violent collisions expands rapidly keeping its almond shape.

IQMD, Au+Au, mid-central
0.6 A.GeV, mid-rapidity, u_{t0}>0.4

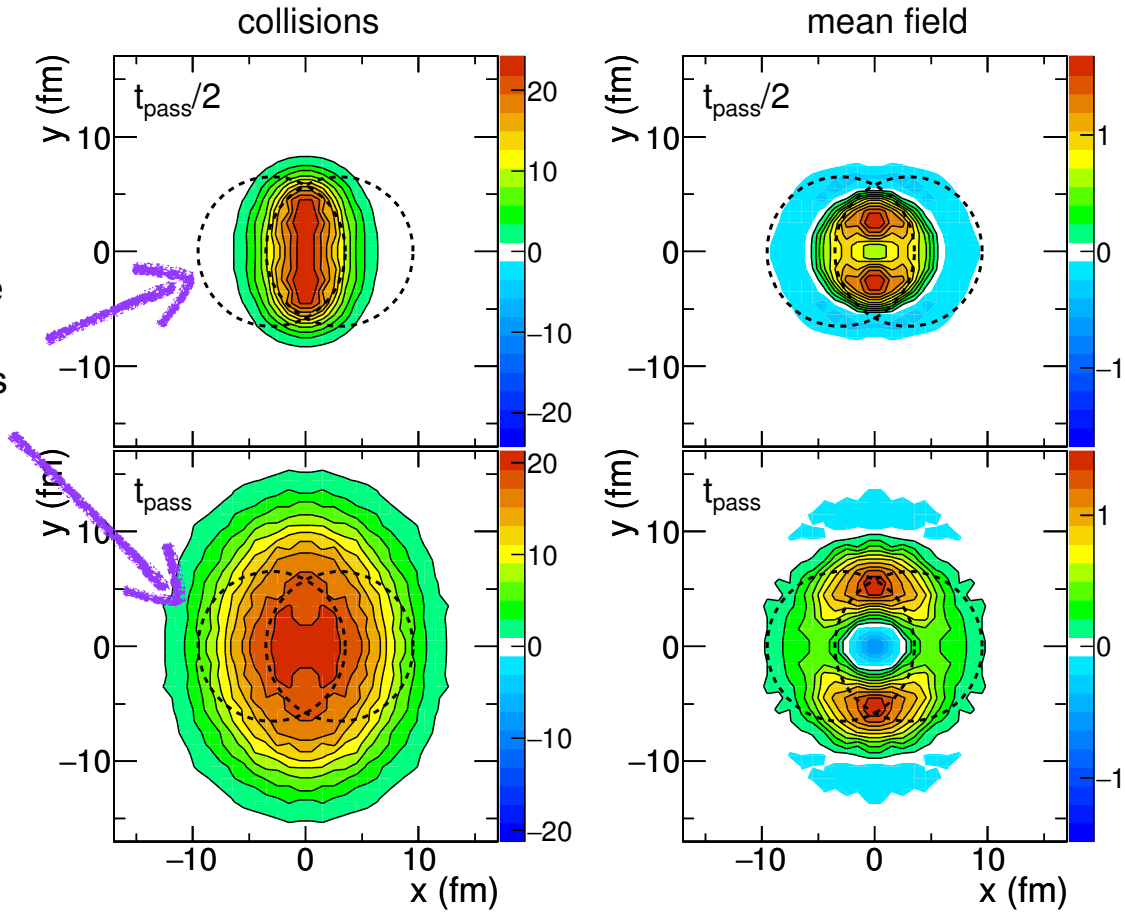

A. Le Fèvre et al., PRC98 (2016) 034901

Origin of elliptic flow: collisions versus mean field

An observable to quantify their respective contribution to it: transverse momentum modification induced projected on the direction of the final momentum:

$$\langle \Delta P_t^o(t) \rangle = \langle \boldsymbol{\Delta P_t}(t) \cdot \frac{\boldsymbol{p}_{final}}{|\boldsymbol{p}_{final}|} \rangle$$

From collisions: about an order of magnitude larger than from mean field, set fast in the overlap zone ⇨ this zone of violent collisions expands rapidly keeping its almond shape.

From mean field: large out-of plane momentum transfer at the tips of the almond shape because here nucleons are between vacuum and the central densest zone ⇨ highest density gradient, largest force ⇨ move in y-direction out of the overlap zone.

IQMD, Au+Au, mid-central
0.6 A.GeV, mid-rapidity, u_{t0}>0.4

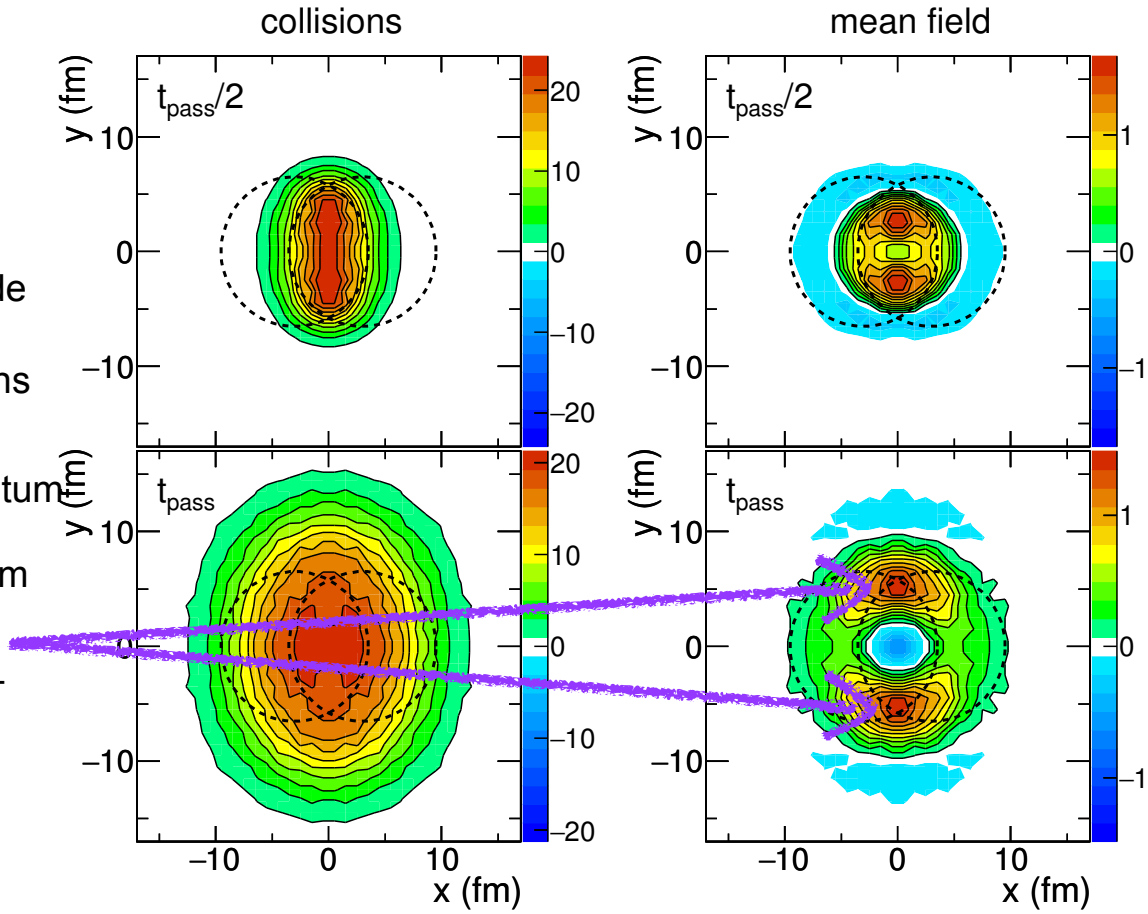

A. Le Fèvre et al., PRC98 (2016) 034901

Origin of elliptic flow: collisions versus mean field

An observable to quantify their respective contribution to it: transverse momentum modification induced projected on the direction of the final momentum:

$$\langle \Delta P_t^o(t) \rangle = \langle \boldsymbol{\Delta P_t}(t) \cdot \frac{\boldsymbol{p}_{final}}{|\boldsymbol{p}_{final}|} \rangle$$

From collisions: about an order of magnitude larger than from mean field, set fast in the overlap zone ⇨ this zone of violent collisions expands rapidly keeping its almond shape.

From mean field: large out-of plane momentum transfer at the tips of the almond shape because here nucleons are between vacuum and the central densest zone ⇨ highest density gradient, largest force ⇨ move in y-direction out of the overlap zone.

Outer blue areas ⇦ attractive potential of the remnant, deceleration.

Inner blue area: inner density decreases and attraction by the moving spectators ⇨ transverse velocity decreases

IQMD, Au+Au, mid-central
0.6 A.GeV, mid-rapidity, u_{t0}>0.4

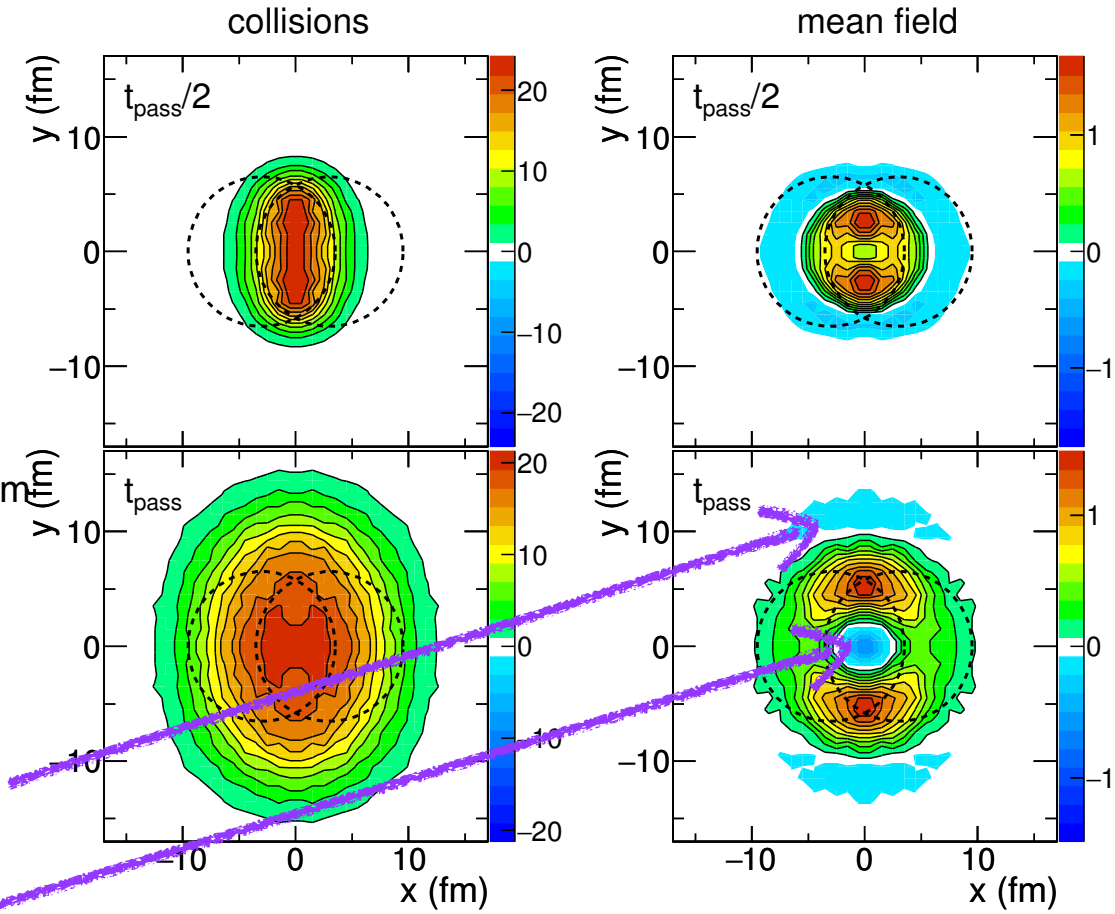

A. Le Fèvre et al., PRC98 (2016) 034901

Origin of elliptic flow: collisions versus mean field

Little difference between 0.6 AGeV and at 1.5 AGeV.

1.5 A.GeV, mid-rapidity, u_{t0}>0.4

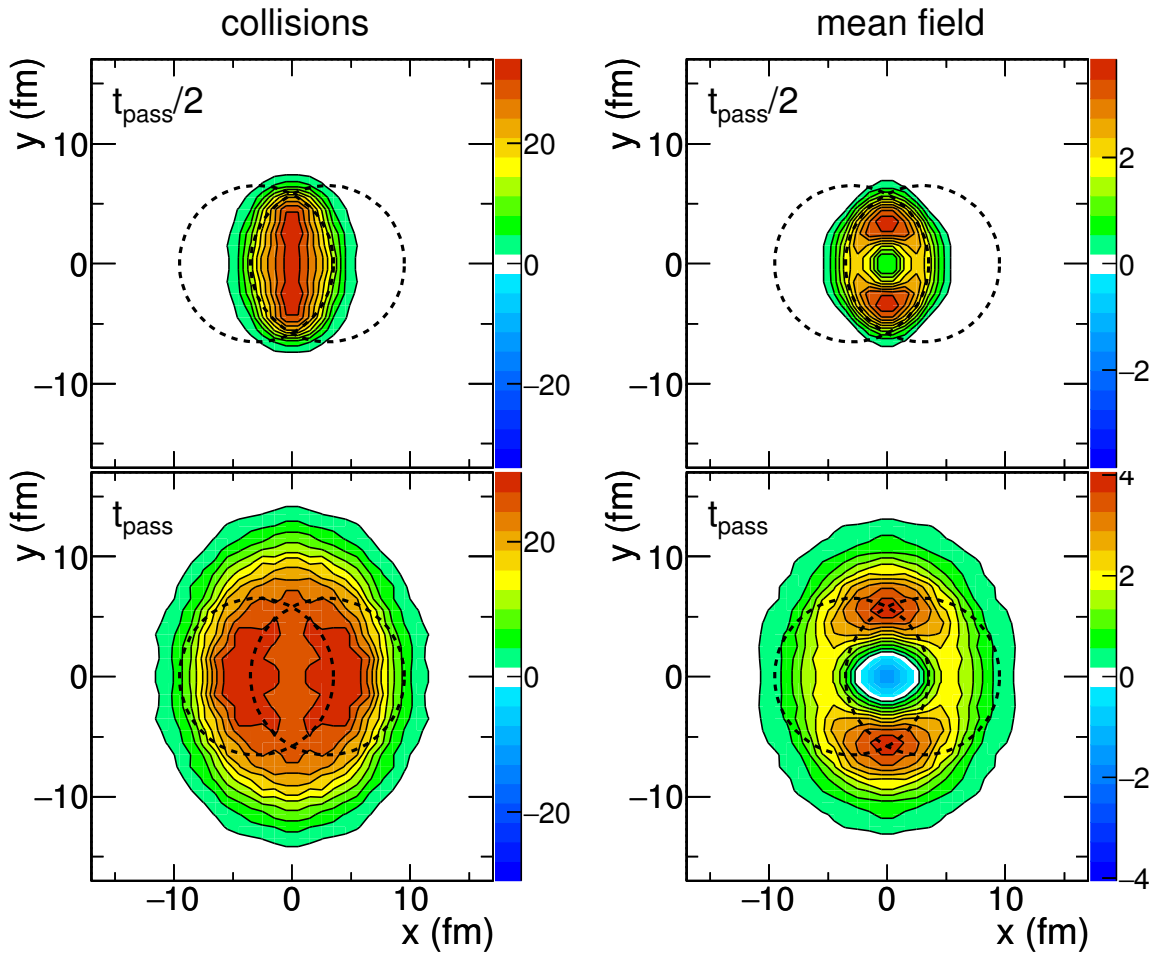

A. Le Fèvre et al., PRC98 (2016) 034901

Origin of elliptic flow: collisions versus mean field

A. Le Fèvre et al., PRC98 (2016) 034901

Origin of elliptic flow: collisions versus mean field

❖ The elliptic flow observed in the reactions around $E_{kin} \approx 1$ AGeV for protons at mid-rapidity
($|y_0| < 0.2$) has two origins:

A. Le Fèvre et al., PRC98 (2016) 034901

Origin of elliptic flow: collisions versus mean field

- The elliptic flow observed in the reactions around $E_{kin} \approx 1$ AGeV for protons at mid-rapidity
($|y_0| < 0.2$) has two origins:
  - the **collisions** of participant nucleons with the **spectator matter**

A. Le Fèvre et al., PRC98 (2016) 034901

Origin of elliptic flow: collisions versus mean field

- The elliptic flow observed in the reactions around $E_{kin} \approx 1$ AGeV for protons at mid-rapidity
($|y_0| < 0.2$) has two origins:
  - the **collisions** of participant nucleons with the **spectator matter**
  - the acceleration of **participants** in the **mean field**.

A. Le Fèvre et al., PRC98 (2016) 034901

Origin of elliptic flow: collisions versus mean field

- The elliptic flow observed in the reactions around $E_{kin} \approx 1$ AGeV for protons at mid-rapidity
($|y_0| < 0.2$) has two origins:
  - the **collisions** of participant nucleons with the **spectator matter**
  - the acceleration of **participants** in the **mean field**.
- The collisional component of v_2 is almost independent of the EoS (due to Pauli blocking),

A. Le Fèvre et al., PRC98 (2016) 034901

Origin of elliptic flow: collisions versus mean field

- The elliptic flow observed in the reactions around $E_{kin} \approx 1$ AGeV for protons at mid-rapidity ($|y_0| < 0.2$) has two origins:
  - the **collisions** of participant nucleons with the **spectator matter**
  - the acceleration of **participants** in the **mean field**.
- The collisional component of v_2 is almost independent of the EoS (due to Pauli blocking),
- The mean field contribution is for a hard EoS (HM) roughly twice as large as that for a soft EoS (SM).

A. Le Fèvre et al., PRC98 (2016) 034901

Origin of elliptic flow: collisions versus mean field

- The elliptic flow observed in the reactions around $E_{kin} \approx 1$ AGeV for protons at mid-rapidity
($|y_0| < 0.2$) has two origins:
  - the **collisions** of participant nucleons with the **spectator matter**
  - the acceleration of **participants** in the **mean field**.
- The collisional component of v_2 is almost independent of the EoS (due to Pauli blocking),
- The mean field contribution is for a hard EoS (HM) roughly twice as large as that for a soft EoS (SM).
- At largest out-of-plane emission (0.6 AGeV$\longleftrightarrow$ max. stopping), for a soft EoS, collisional and mean field contributions are about equal,

A. Le Fèvre et al., PRC98 (2016) 034901

Origin of elliptic flow: collisions versus mean field

- The elliptic flow observed in the reactions around $E_{kin} \approx 1$ AGeV for protons at mid-rapidity
($|y_0| < 0.2$) has two origins:
  - the **collisions** of participant nucleons with the **spectator matter**
  - the acceleration of **participants** in the **mean field**.
- The collisional component of v_2 is almost independent of the EoS (due to Pauli blocking),
- The mean field contribution is for a hard EoS (HM) roughly twice as large as that for a soft EoS (SM).
- At largest out-of-plane emission (0.6 AGeV$\longleftrightarrow$ max. stopping), for a soft EoS, collisional and mean field contributions are about equal,
- In all other cases the contribution of the mean field dominates.

A. Le Fèvre et al., PRC98 (2016) 034901

Origin of elliptic flow: collisions versus mean field

- The elliptic flow observed in the reactions around $E_{kin} \approx 1$ AGeV for protons at mid-rapidity
($|y_0| < 0.2$) has two origins:
  - the **collisions** of participant nucleons with the **spectator matter**
  - the acceleration of **participants** in the **mean field**.
- The collisional component of v_2 is almost independent of the EoS (due to Pauli blocking),
- The mean field contribution is for a hard EoS (HM) roughly twice as large as that for a soft EoS (SM).
- At largest out-of-plane emission (0.6 AGeV$\longleftrightarrow$ max. stopping), for a soft EoS, collisional and mean field contributions are about equal,
- In all other cases the contribution of the mean field dominates.
- Mean field out-of-plane flow comes from **nucleons close to the tips of fireball**: strongest density gradient in y-direction

A. Le Fèvre et al., PRC98 (2016) 034901

Origin of elliptic flow: collisions versus mean field

- The elliptic flow observed in the reactions around $E_{kin} \approx 1$ AGeV for protons at mid-rapidity
($|y_0| < 0.2$) has two origins:
  - the **collisions** of participant nucleons with the **spectator matter**
  - the acceleration of **participants** in the **mean field**.
- The collisional component of v_2 is almost independent of the EoS (due to Pauli blocking),
- The mean field contribution is for a hard EoS (HM) roughly twice as large as that for a soft EoS (SM).
- At largest out-of-plane emission (0.6 AGeV$\longleftrightarrow$ max. stopping), for a soft EoS, collisional and mean field contributions are about equal,
- In all other cases the contribution of the mean field dominates.
- Mean field out-of-plane flow comes from **nucleons close to the tips of fireball**: strongest density gradient in y-direction
- This effect is amplified if one selects particles with a high transverse velocity.

A. Le Fèvre et al., PRC98 (2016) 034901

Elliptic flow: densities probed by FOPI

Determining densities probed by an experiment with a given observable is capital !

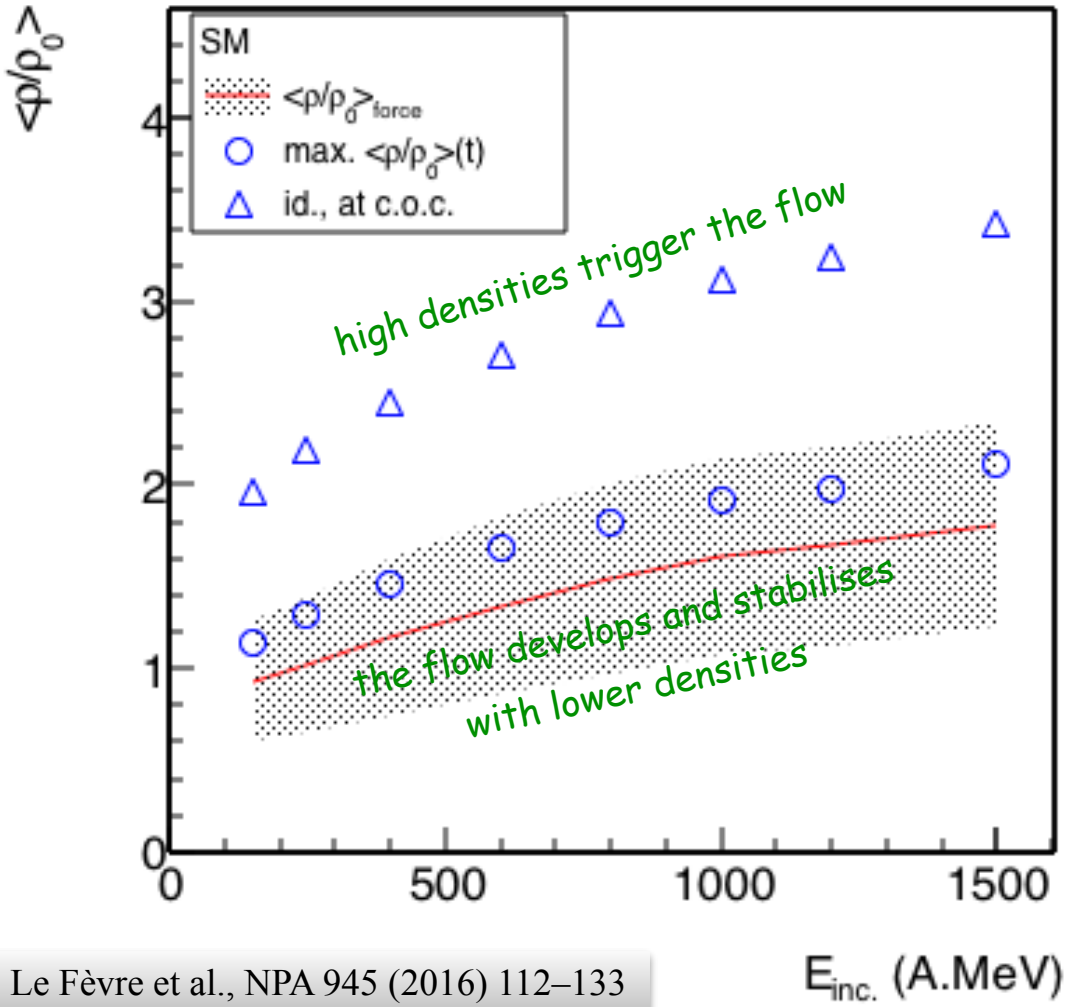

A. Le Fèvre et al., NPA 945 (2016) 112–133

- In the QMD model, the EOS must be correct over a broad range of densities in order to predict the observed elliptic flow.
- The density range, relevant to the EOS evidenced by the FOPI Collaboration, spans in the range $\rho \simeq (1-3)\,\rho_0$.

Elliptic flow method: FOPI EoS constraints

- K_0 as from FOPI flow data

$$IQMD -> K_0 = 190 \pm 30\ MeV$$

[A. Le Fèvre et al., NPA945(2016)112-133]

$$UrQMD -> K_0 = 220 \pm 40\ MeV$$

[Y. Wang et al., PLB-778(2018)207-212]

$$dcQMD -> K_0 = 230^{+9}_{-11}\ MeV$$

[M.D. Cozma, PRC 110 (2024) 0649111]

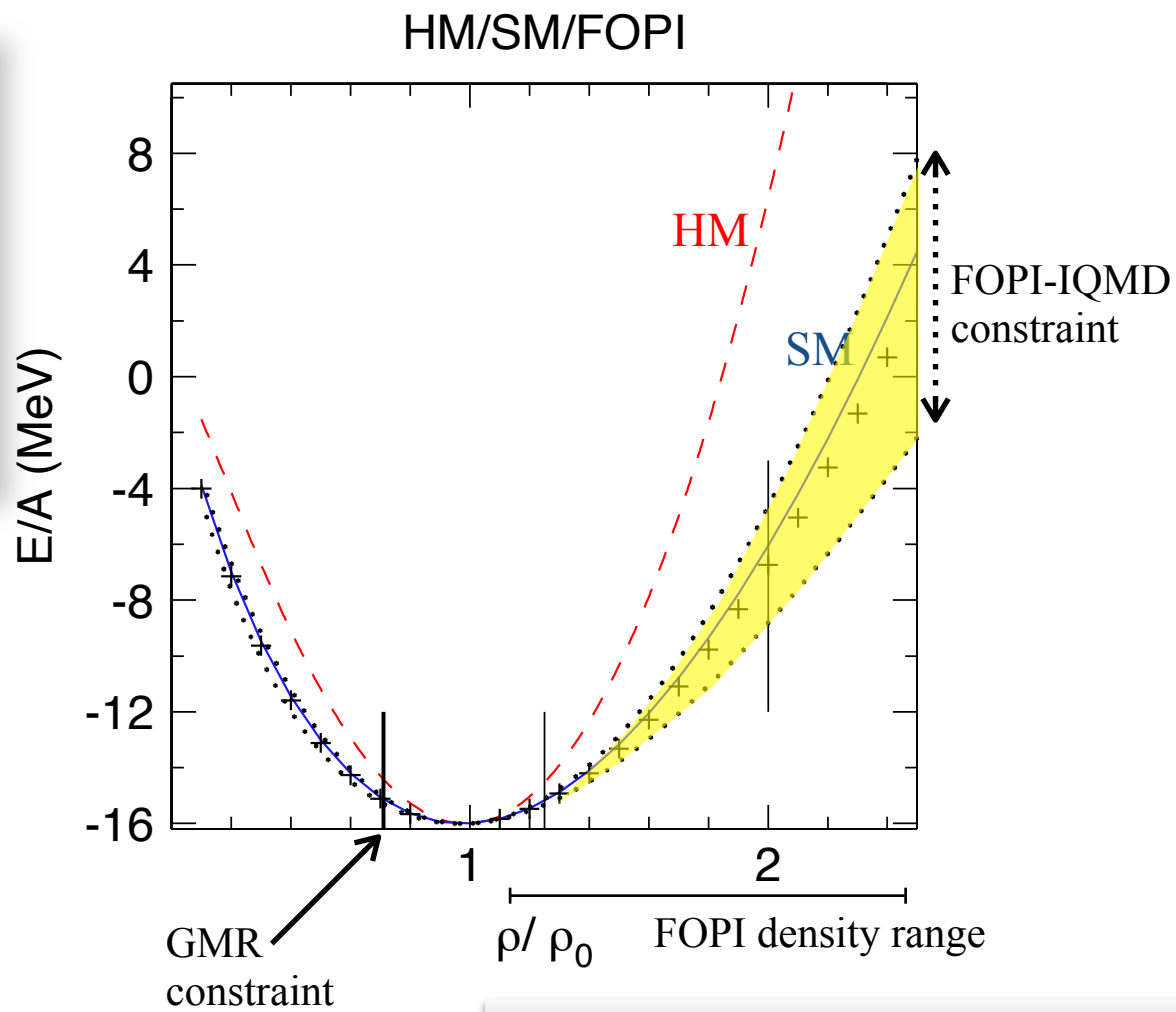

A. Le Fèvre et al., NPA 945 (2016) 112–133

Elliptic flow and symmetry energy constraint with ASY-EOS I

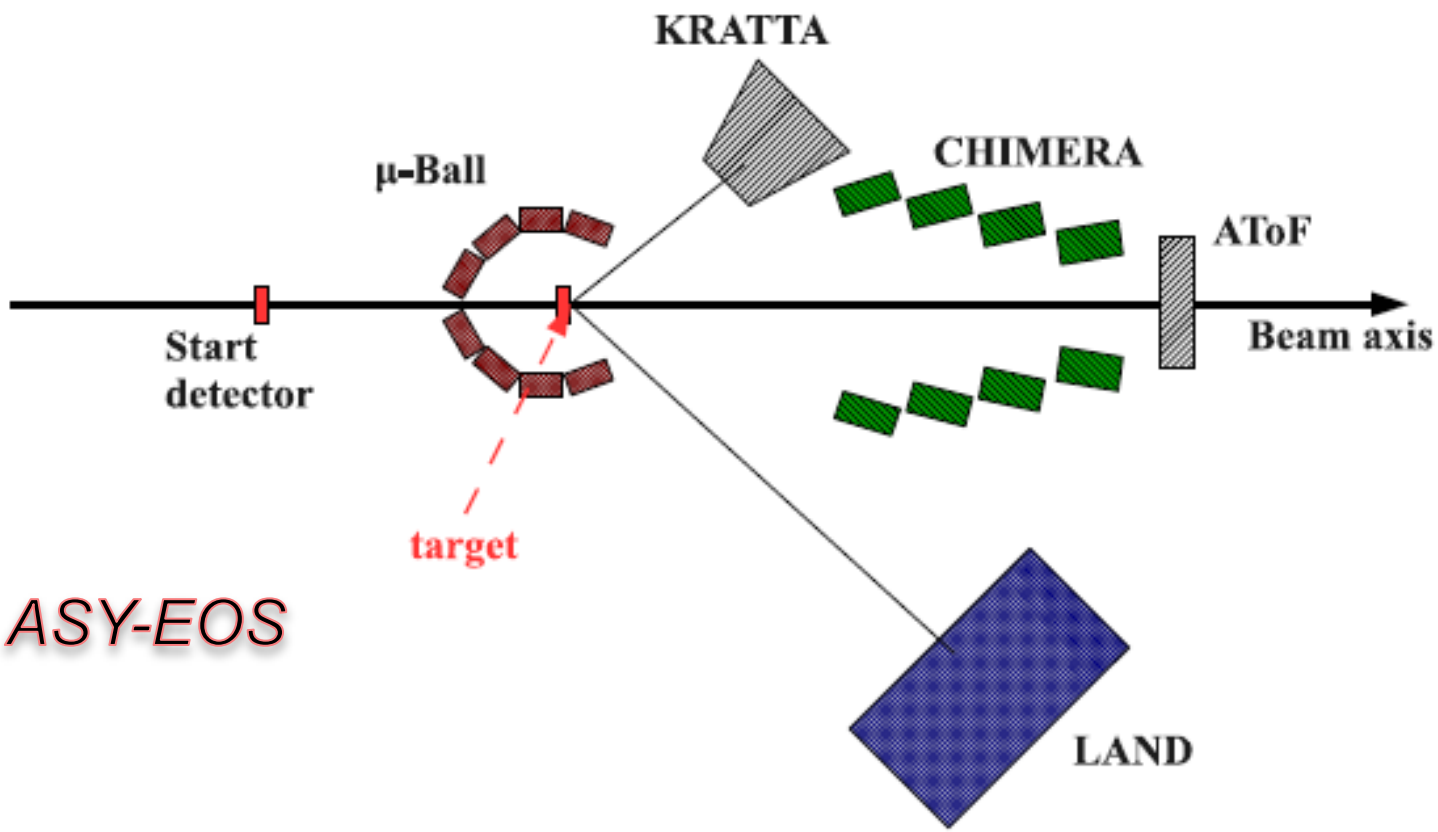

➢ 400A MeV Au+Au, ^{96}Zr+Zr, ^{96}Ru+Ru at GSI (2011)

Elliptic flow and symmetry energy constraint with ASY-EOS I

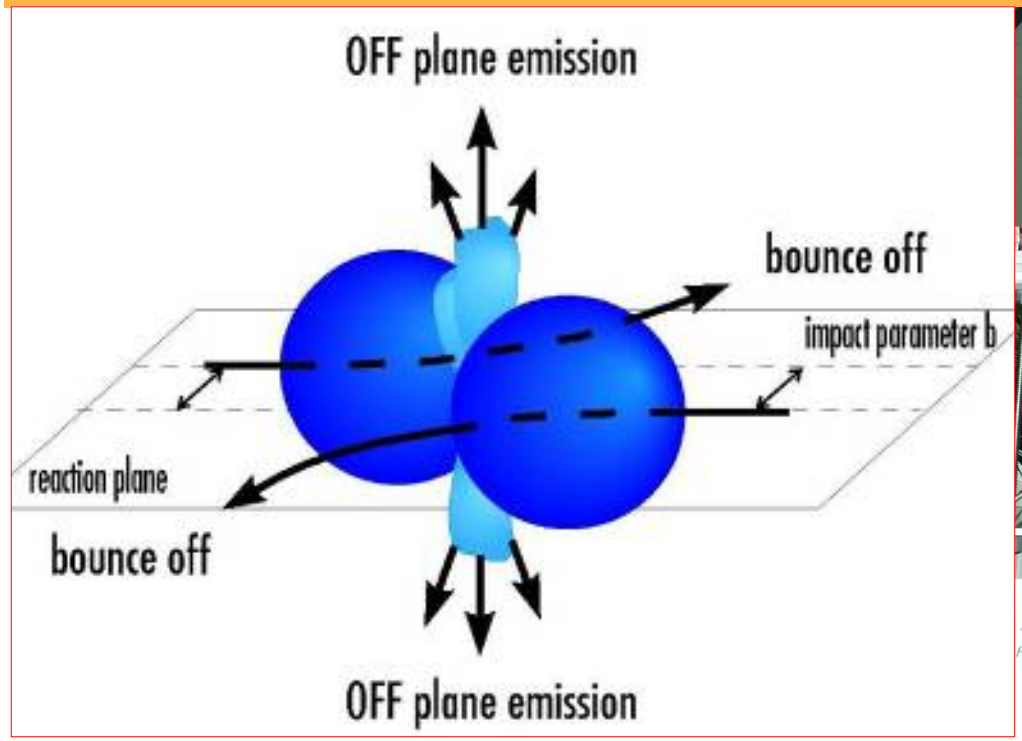

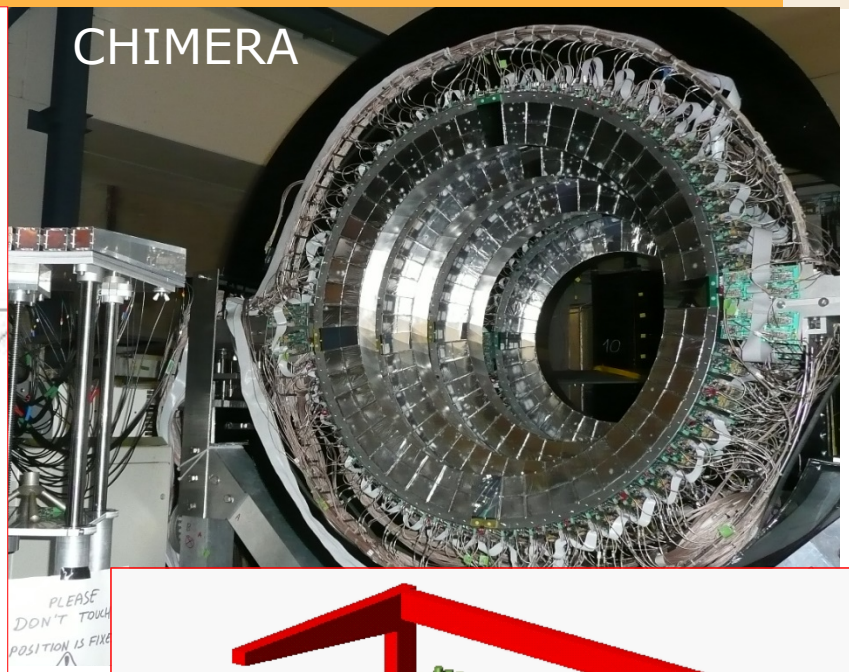

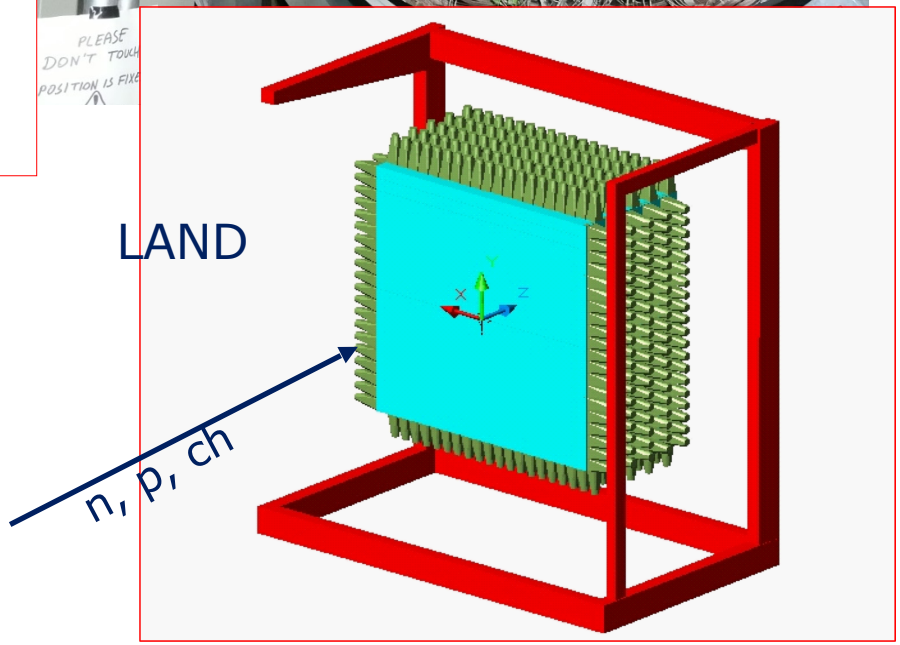

tested with existing **FOPI-LAND** data
^{197}Au + ^{197}Au @ 400 A MeV
Russotto+ PLB 697 (2011)

ASY-EOS experiment in 2011
^{197}Au + ^{197}Au @ 400 A MeV
Russotto+ PRC 94 (2016)

Elliptic flow and symmetry energy constraint with ASY-EOS I

Differential elliptic flow v_2 of n/p

UrQMD* (Q. Li et al.) predicts:

"hard" $E_{sym}(\rho)$ protons unchanged

→

"soft" $E_{sym}(\rho)$ neutron and proton flow inverted

Towards model invariance:

tested stability with different models:

- ➢ soft vs. hard EoS: $190 < K_0 < 260$ MeV
- ➢ density dependance of $\sigma_{NN,elastic}$
- ➢ asymmetry dependance of $\sigma_{NN,elastic}$
- ➢ optical potential
- ➢ momentum dependence of isovector potential

M.D. Cozma et al.,PRC 88 (2013) 044912,
PRC 110 (2024) 0649111
P. Russotto et al., PLB 267 (2010)
Y. Wang et al.,PRC 89, 044603 (2014)

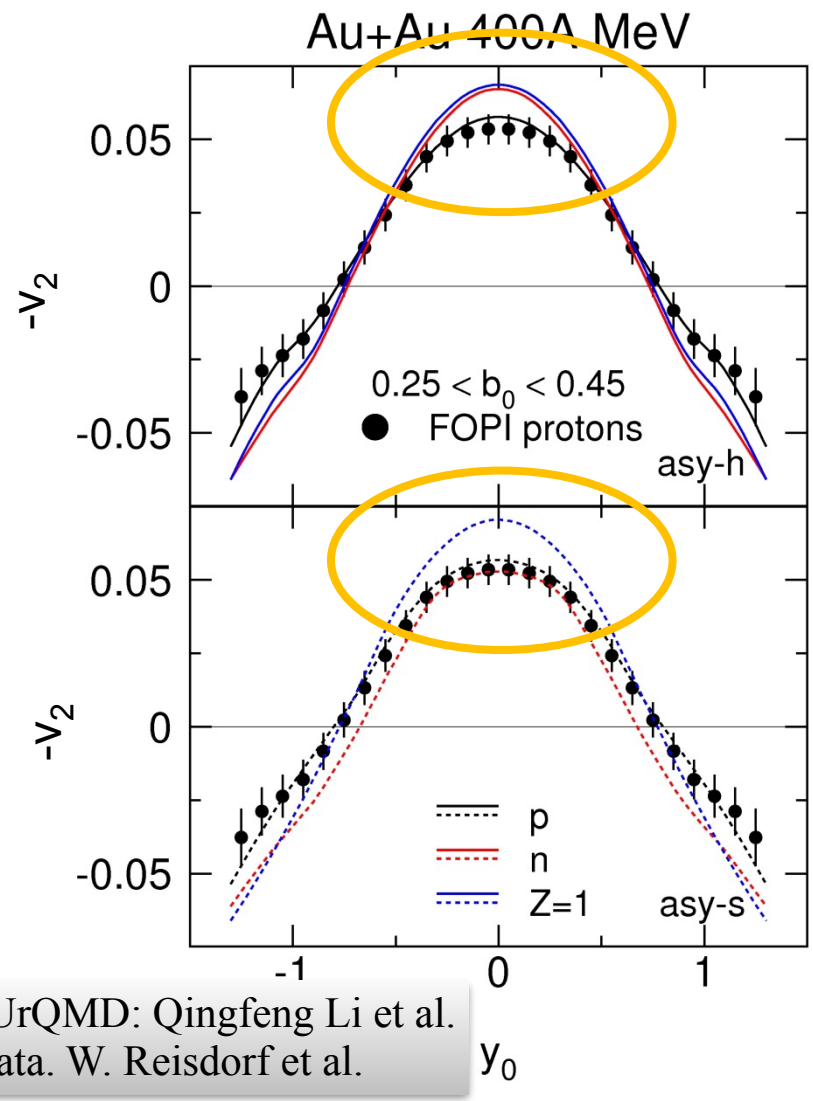

*UrQMD: Qingfeng Li et al.
Data. W. Reisdorf et al.

Elliptic flow method: high densities ASY-EOS

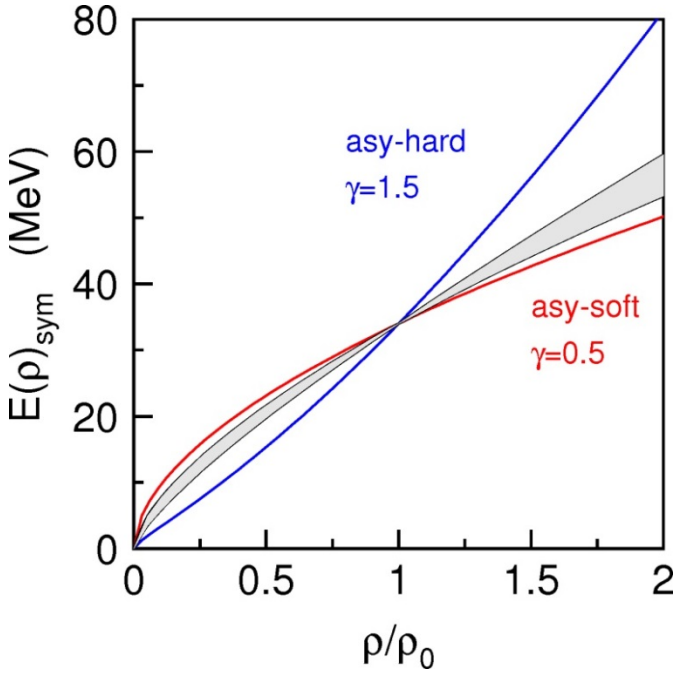

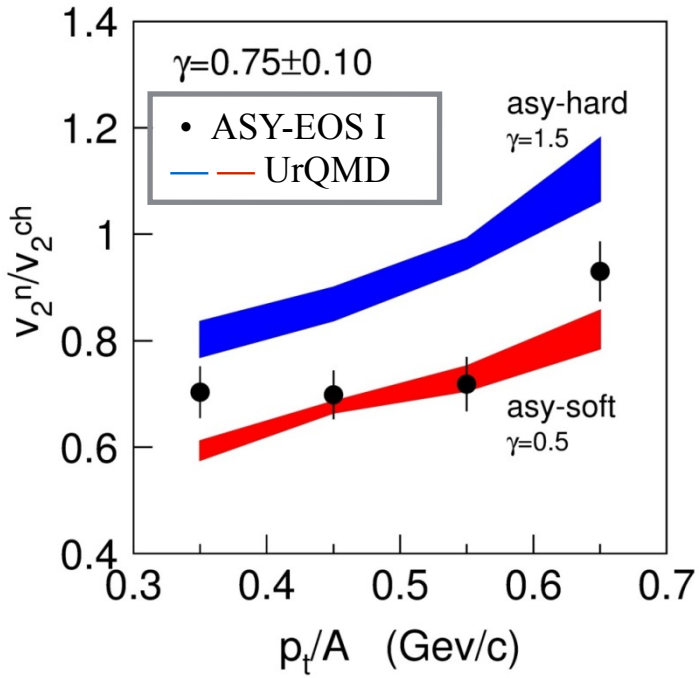

P. Russotto et al., PRC (2017)

- parametrization for E_{asy} used in the UrQMD model:
  $E_{sym} = E_{sym}^{pot} + E_{sym}^{kin} = 22\ \text{MeV}\cdot(\rho/\rho_0)^{\gamma} + 12\ \text{MeV}\cdot(\rho/\rho_0)^{2/3}$
- systematic errors corrected: $\gamma = 0.72 \pm 0.19$
- slope parameter: $L = 72 \pm 13$ MeV, $E_{sym}(\rho_0) = 34$ MeV
- slope parameter: $L = 63 \pm 11$ MeV, $E_{sym}(\rho_0) = 31$ MeV

- A more recent analysis of M.D. Cozma with dcQMD has concluded
  $L = 63^{+10}_{-13}\ MeV, E_{sym}(\rho_0) = 35 \pm 1\ MeV$

M.D. Cozma, PRC 110 (2024) 0649111

ASY-EOS: neutron vs charged-particle elliptic flow ratio

sensitivity to density

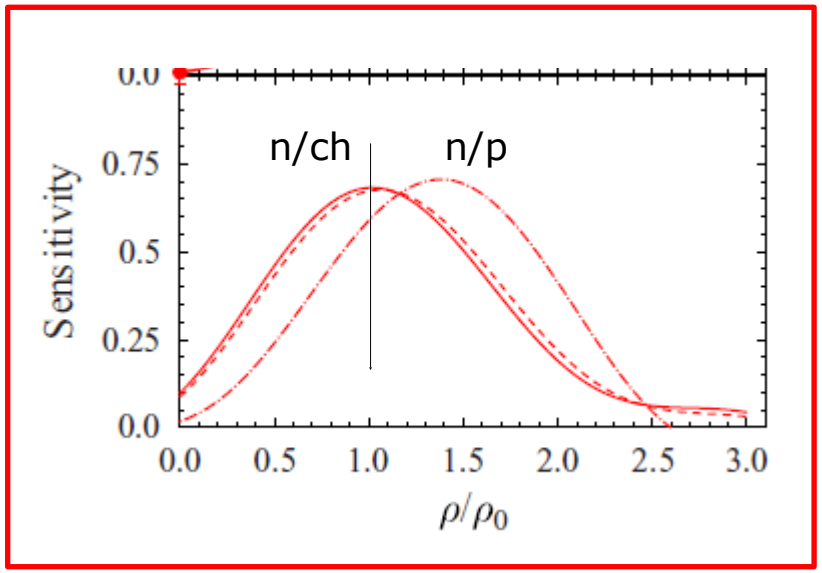

density probed extends to 2.5 ρ_0
maximum near **saturation density**

P. Russotto+ PRC 94, 034608 (2016)

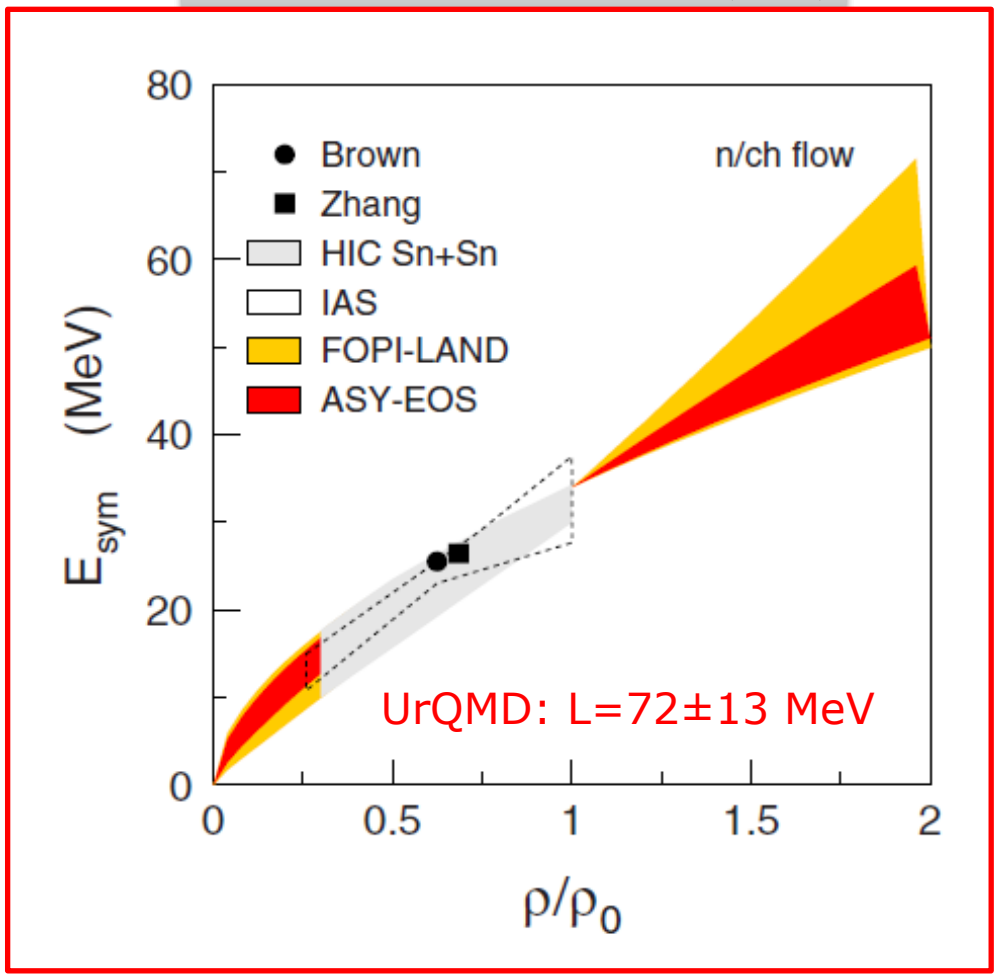

Synthesis EoS: FOPI and ASY-EOS I

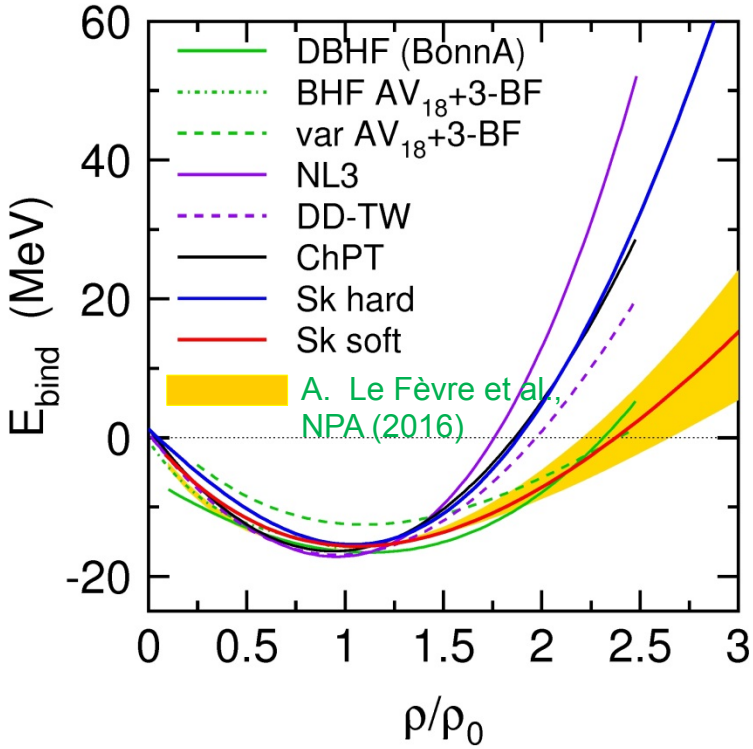

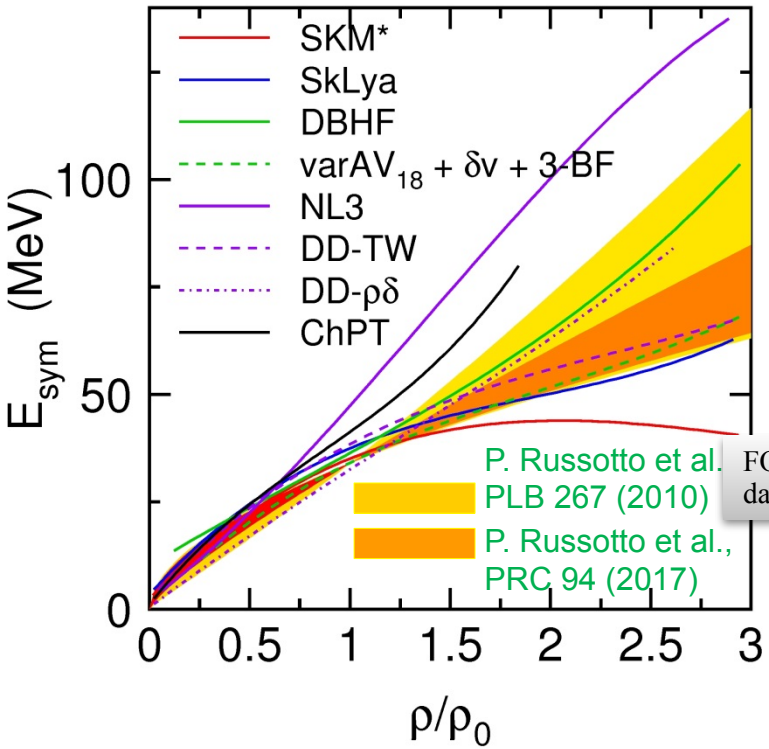

Synthesis EoS: FOPI and ASY-EOS I

M.D. Cozma, PRC 110 (2024) 0649111

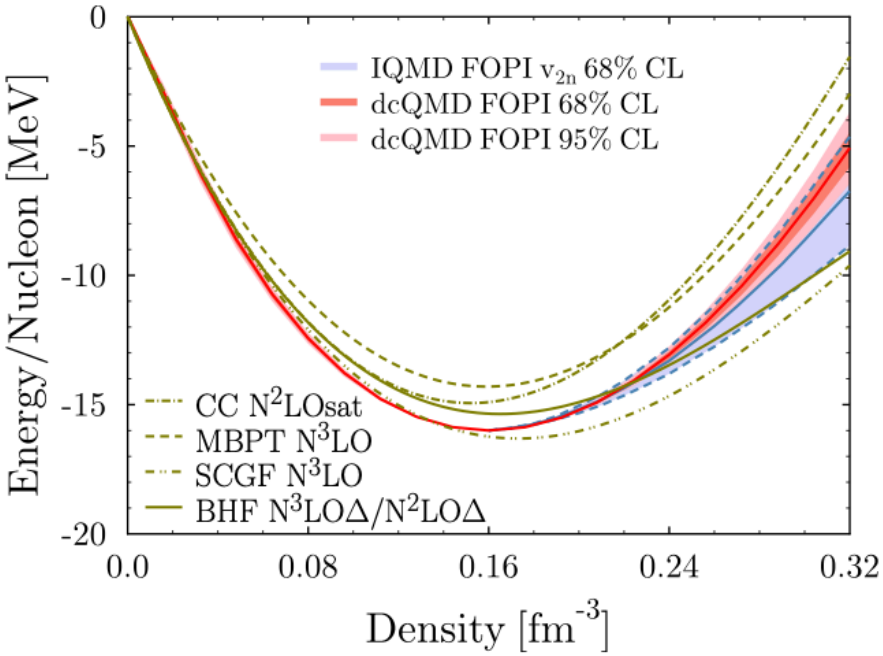

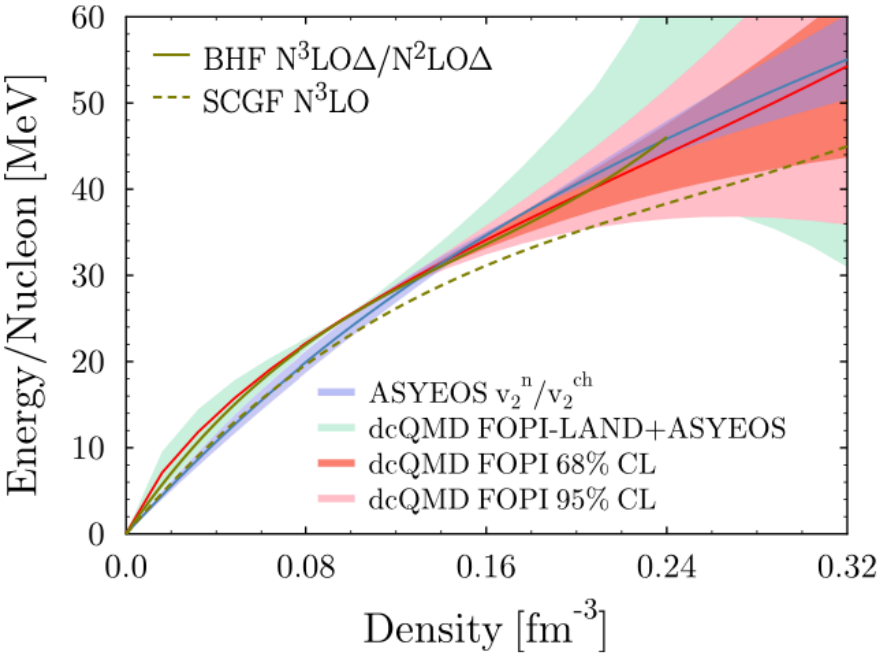

Cf. M.D. Cozma's talk on Thursday

FOPI - ASY-EOS EoS constraints and neutron stars

Reed Essick at NuSym22 in Catania

ASY-EOS:
neutron star pressure
for asymmetry δ = 0.9
$P(\rho_0) = 3.4 \pm 0.6$ MeV/fm^3

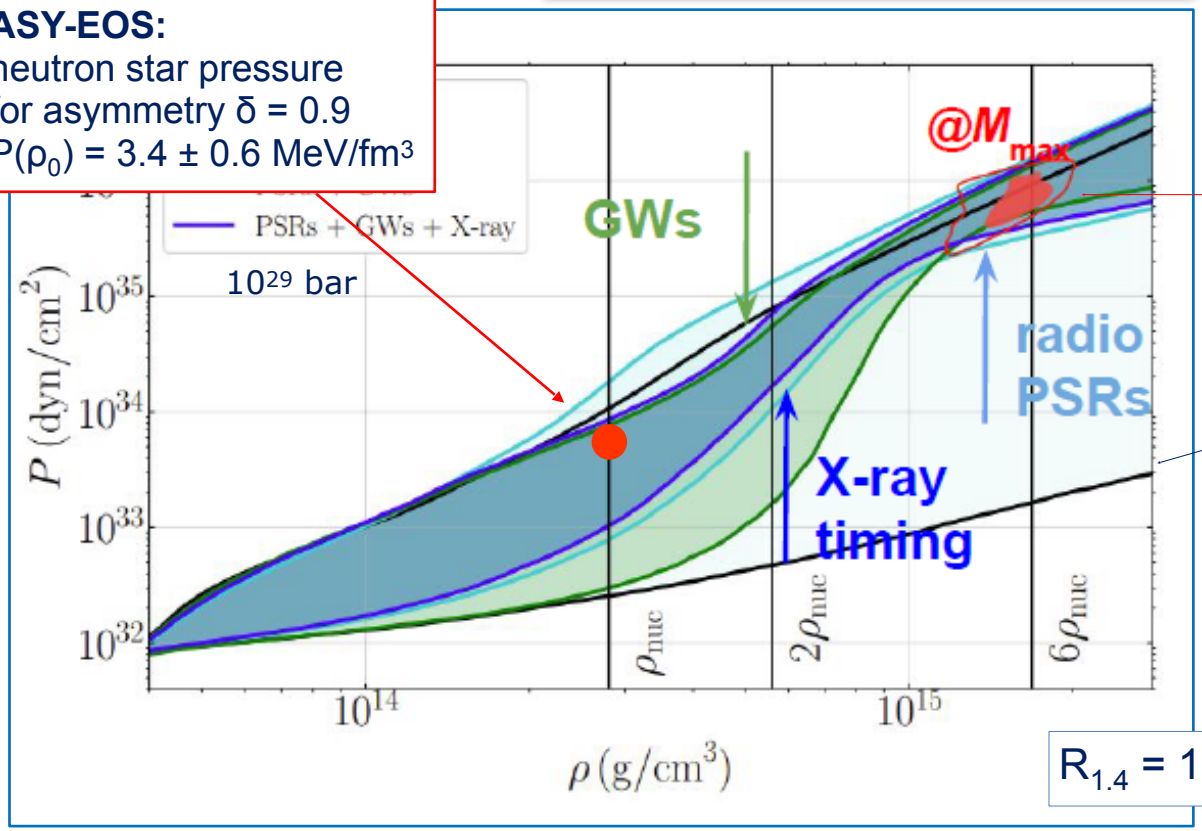

Legred+, PRD 104, 063003 (2021)

50%/90% contours

model-agnostic prior

$R_{1.4} = 12.6 \pm 1.1$ km (68%)

$R_{1.4}P_{sat}^{-1/4} = 9.5 \pm 0.5$ => $R_{1.4} = 12.9 \pm 0.6$ km ± 0.7 km (68%)
(stat.) (correl.)

for ASY-EOS: Russotto+, PRC 94, 034608 (2016)
for correlation: Lattimer, arXiv:2308.08001

Cf. W. Trautmann's talk on Wednesday

Combining heavy-ion experiments, astrophysical observations, and nuclear theory

Nature 606, 276 (2022)

Article

Constraining neutron-star matter with microscopic and macroscopic collisions

https://doi.org/10.1038/s41586-022-04750-w

Received: 13 July 2021

Accepted: 11 April 2022

Published online: 8 June 2022

Open access

Check for updates

Sabrina Huth[1,2,13], Peter T. H. Pang[3,4,13], Ingo Tews[5], Tim Dietrich[6,7], Arnaud Le Fèvre[8], Achim Schwenk[1,2,9], Wolfgang Trautmann[8], Kshitij Agarwal[10], Mattia Bulla[11], Michael W. Coughlin[12] & Chris Van Den Broeck[3,4]

Interpreting high-energy, astrophysical phenomena, such as supernova explosions or neutron-star collisions, requires a robust understanding of matter at supranuclear densities. However, our knowledge about dense matter explored in the cores of neutron stars remains limited. Fortunately, dense matter is not probed only in

iments.

messenger

11 authors from nuclear theory, heavy ion reactions, and astrophysics

Bayesian inference as in Dietrich+, Science 370, 1450 (2020)

χEFT prior + HIC + astro

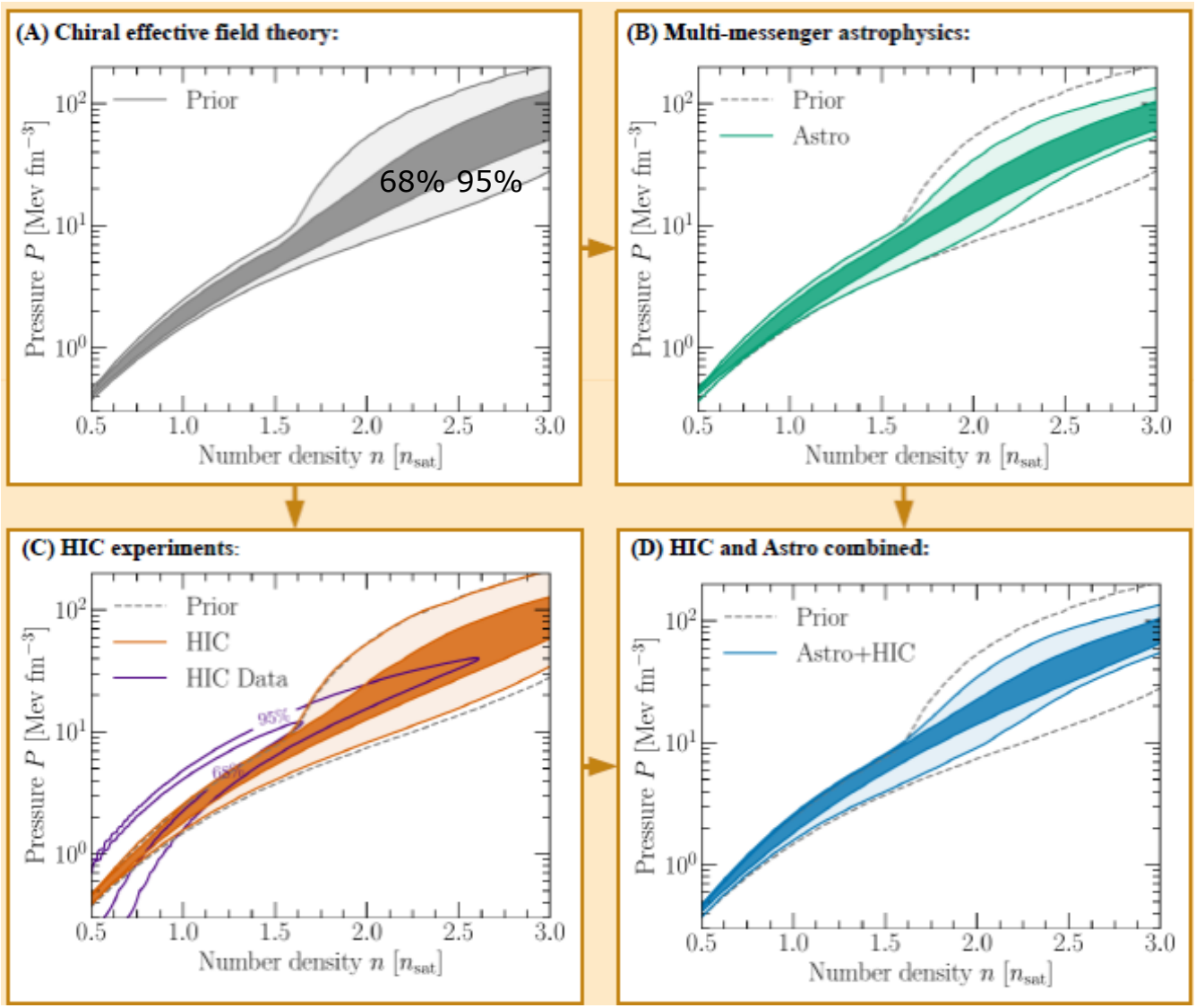

2022 Huth+ Nature
Fig. 1

neutron star matter

contours at
68% and 95%
credibility

prior:
χEFT up to 1.5 ρ_0
$M_{max} \geq 1.9\ M_{sun}$

astro:
GW170817
+kilonova
GW190425
NICER 2 stars
XMM-Newton
$M_{max} \leq 2.17\ M_{sun}$

HIC:
PNM: ASY-EOS
SNM: FOPI, AGS

Constraints from heavy-ion collisions

Huth, Pang et al.,

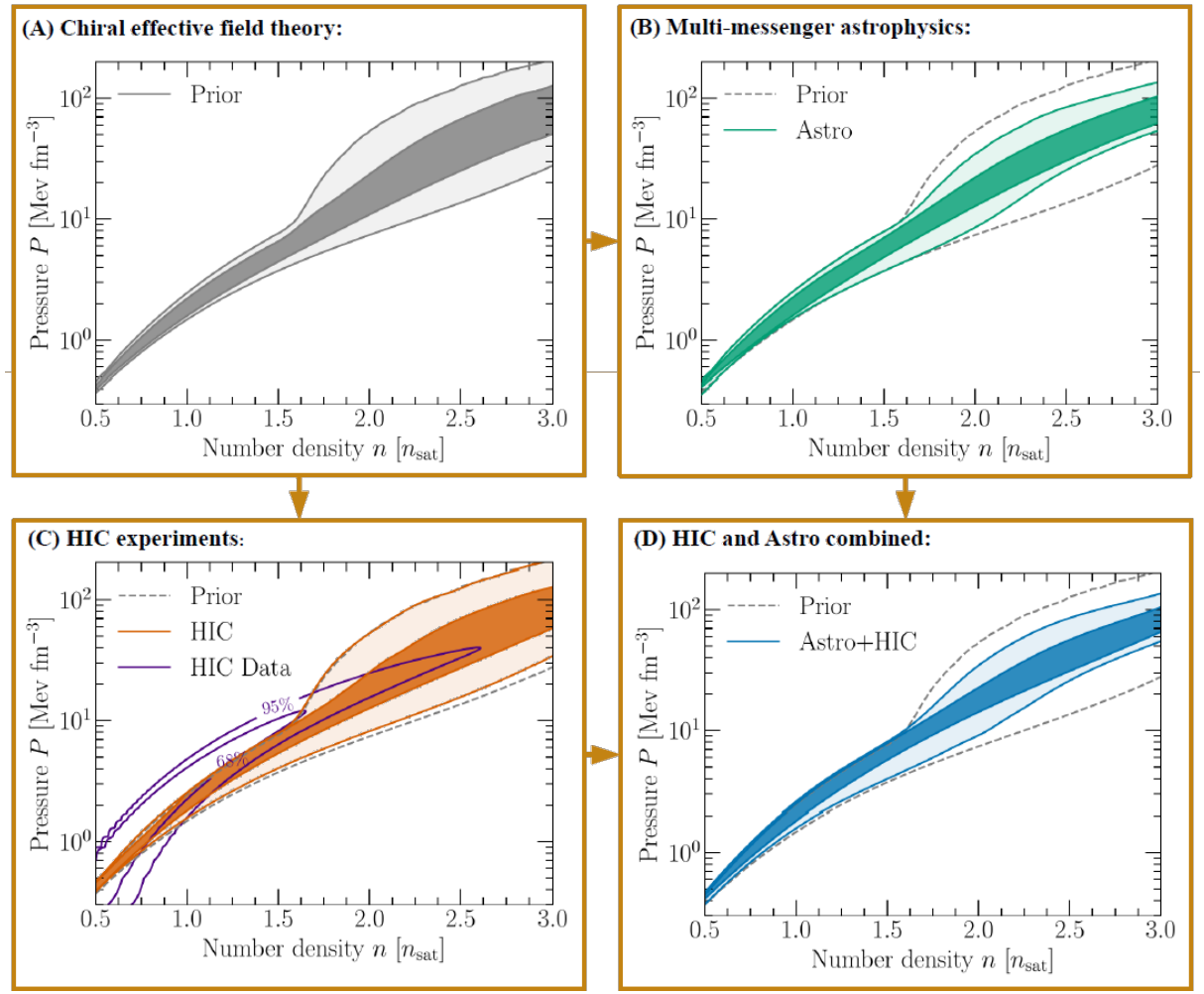

Constraints from heavy-ion collisions

Huth, Pang et al.,

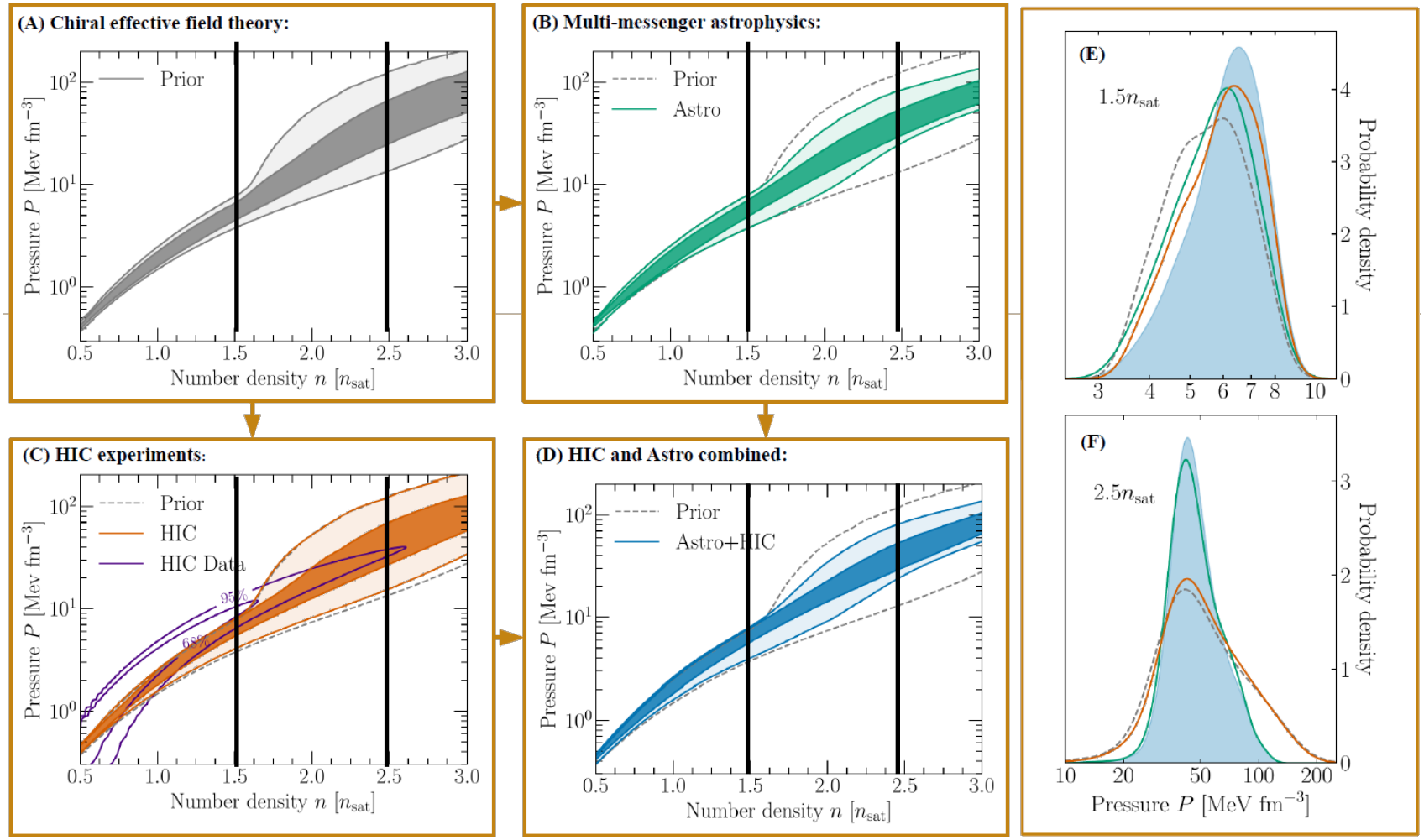

Influence of the choice of the prior

nature astronomy

Article

https://doi.org/10.1038/s41550-023-02161-z

Determination of the equation of state from nuclear experiments and neutron star observations

Received: 22 February 2023

Accepted: 6 November 2023

Published online: 05 January 2024

Chun Yuen Tsang[1,2], ManYee Betty Tsang[1,2], William G. Lynch[1,2], Rohit Kumar[1] & Charles J. Horowitz[1,3]

Influence of the choice of the prior

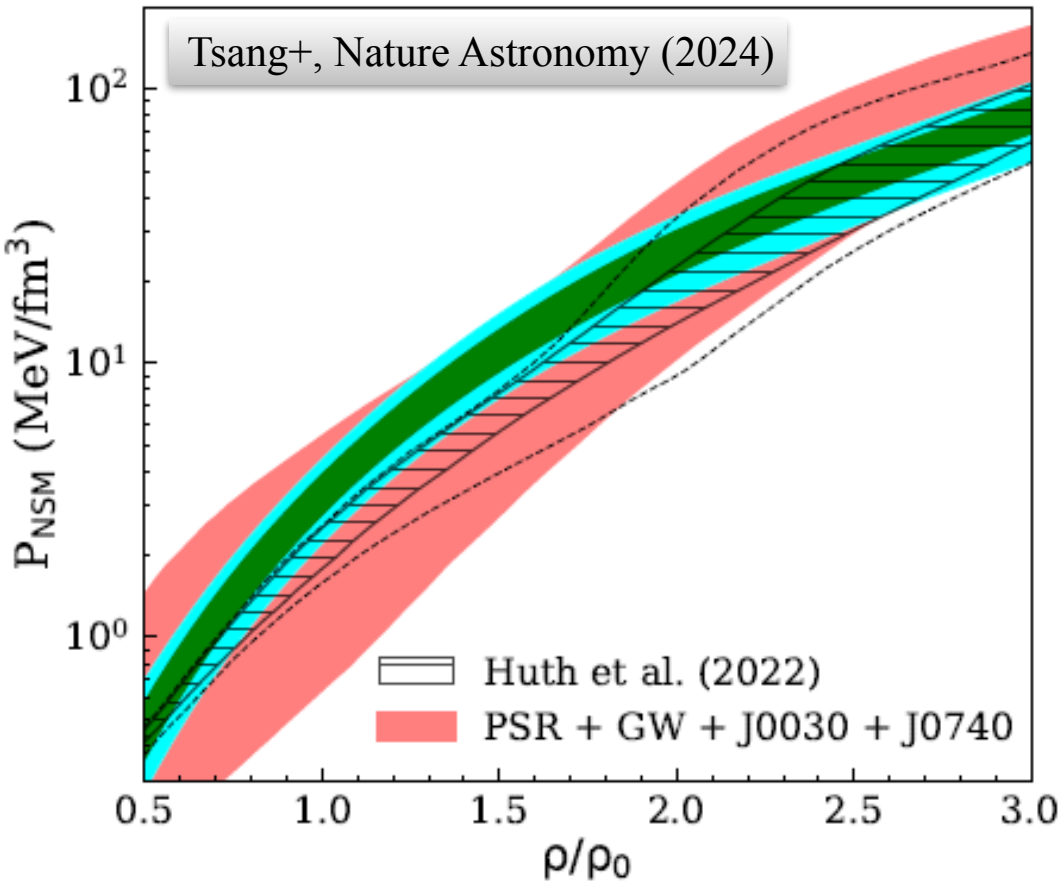

Legred et al., Phys. Rev. D 104, 063003 (2021)

- Non-parametric equation of states as priors.
- Astrophysical observations are used as constraints

Huth, Pang et al., Nature 606, 279 (2022)

- Prior distribution from the Chiral Effective Field theory (up to $1.5n_0$); constant speed of sound model $>1.5n_0$.
- Include HIC(FOURPI) & astrophysical observations as constraints

χEFT seems to generate a **bias** as a prior,
forcing artificially the posterior EoS to be **too soft** in the $0.5 - 1.5\rho_0$ density range

R3B - ASY-EOS II experiment (Cave C, March 2025)

Supported by European Union's Horizon Europe and Horizon 2020 Research and Innovation programmes under Grant Agreements no. 101057511 (EURO-LABS) and no. 824093 (STRONG2020)

- **Goal:** measure the **symmetry energy** of nuclear matter at **high density** ($\gg \rho_0$, world record with HIC) and with **high precision**, to constrain **neutron star properties** (maximum mass, radius, pressure versus density relation)

- **Method:** comparison of the strength of the **out-of-plane emission** (« elliptic flow ») of **protons** and **neutrons** in **heavy- and neutron-rich-ion collisions at relativistic incident energies**

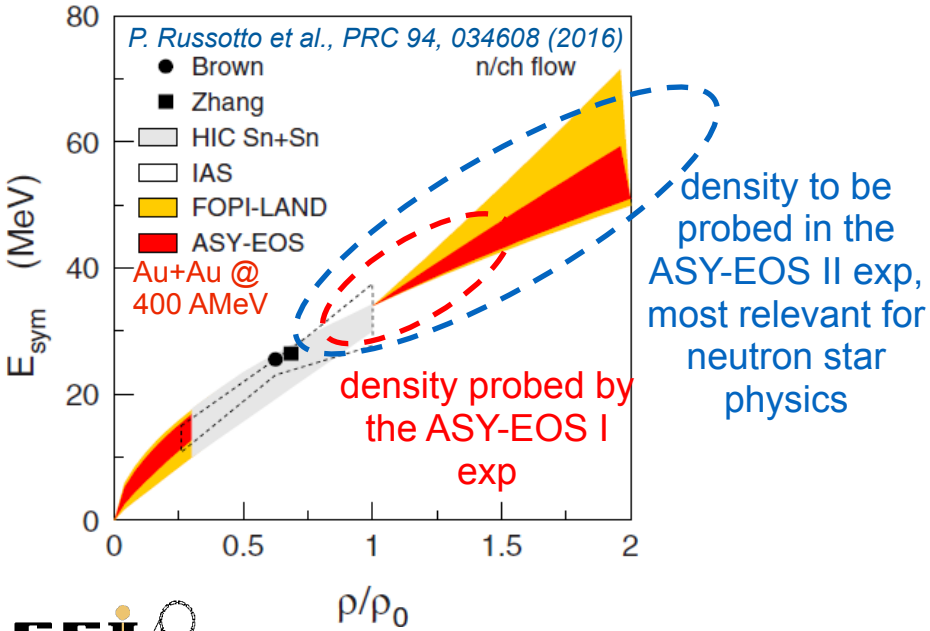

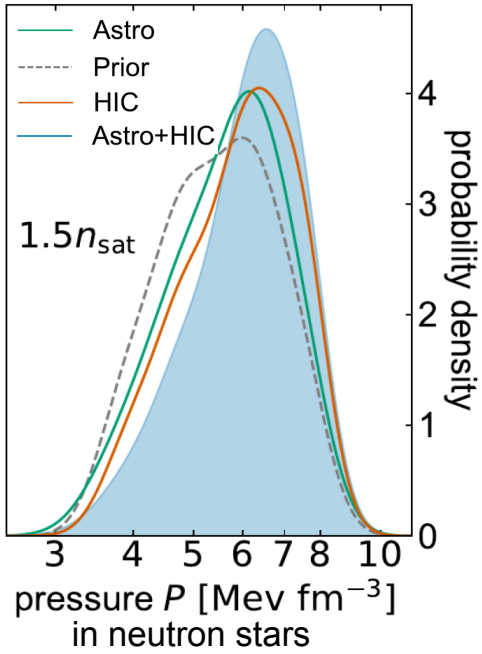

Huth, Pang et al., Nature 606 (2022)

- **March 2025 measurements at GSI Darmstadt**:
  - Au+Au @ 280, 400, 600, 1000A MeV.
  - 10^5 pps, high multiplicity (>80)
  - precise reaction plane determination
  - large neutron and proton acceptance
  - optimised (macro & micro-) spill structure allowed about 30% more statistics.
  - large statistics (about 100M clean events)

R3B - ASY-EOS II experiment (Cave C, March 2025)

Reaction plane: KRAB, CHIMERA
Impact parameter: TOFD
Neutron/proton flow: TOFD+NeuLAND

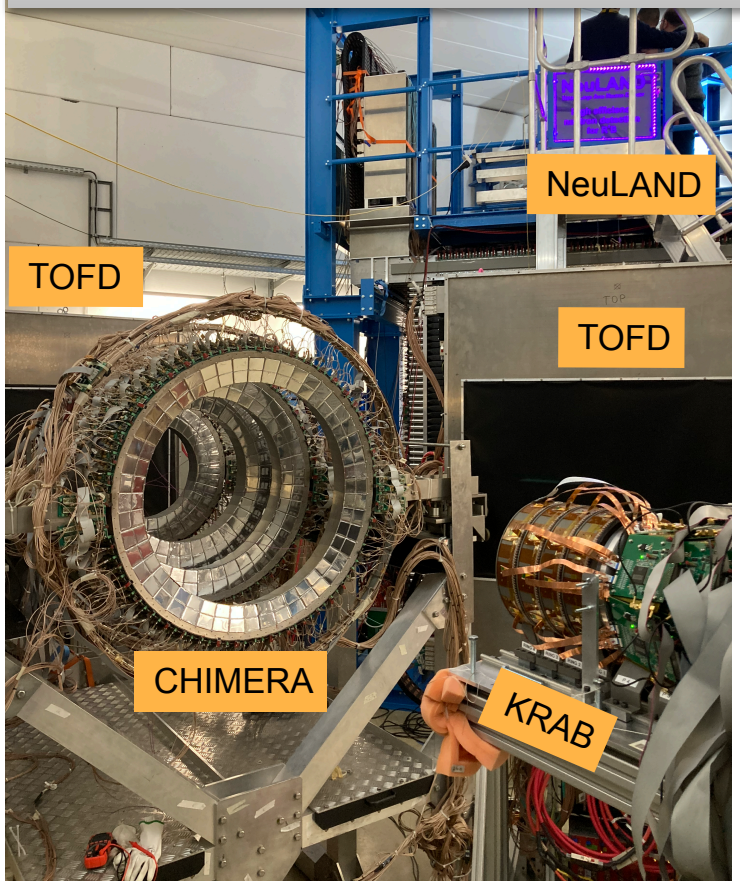

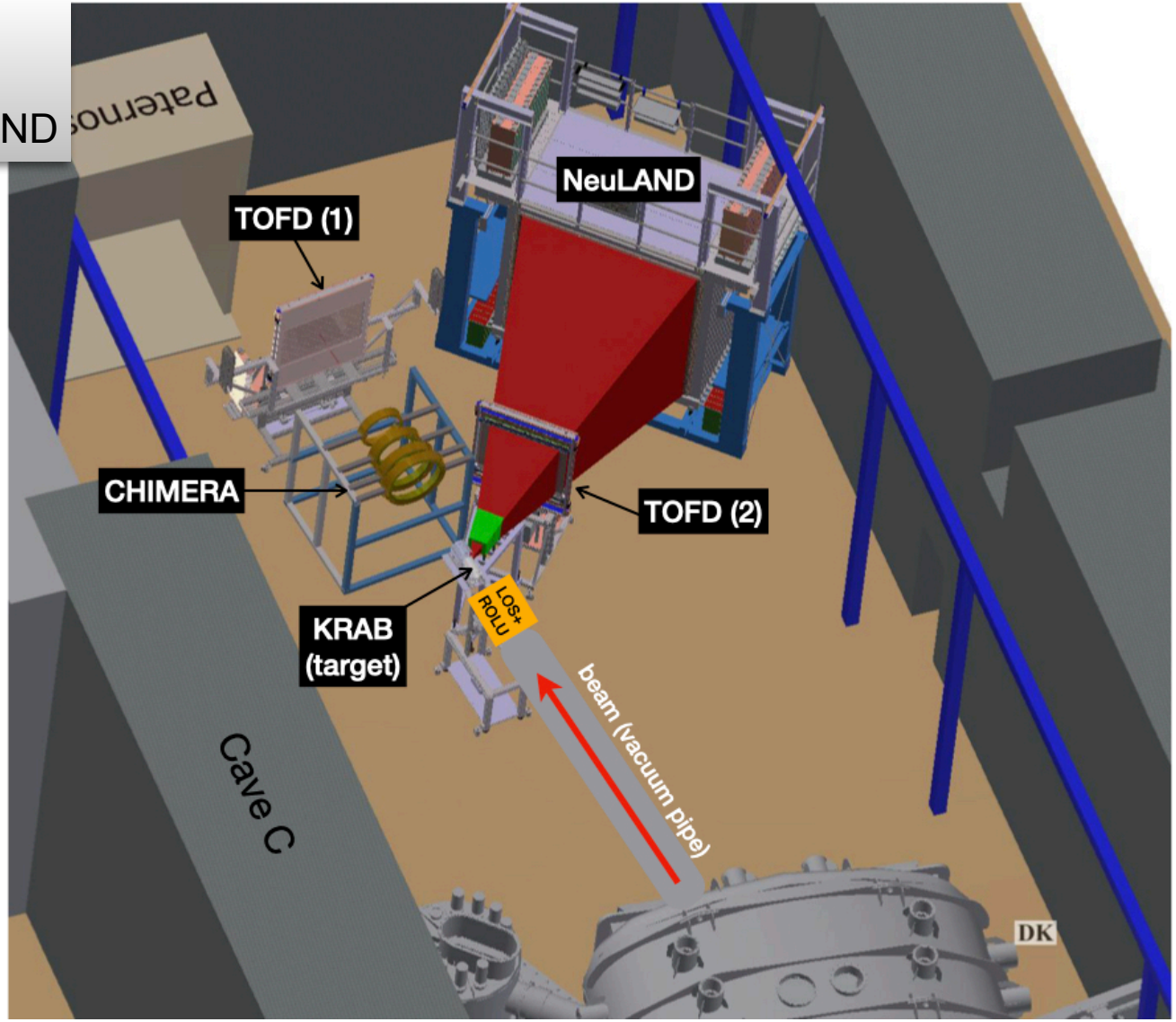

R3B - ASY-EOS II experiment (Cave C, March 2025)

Statistics

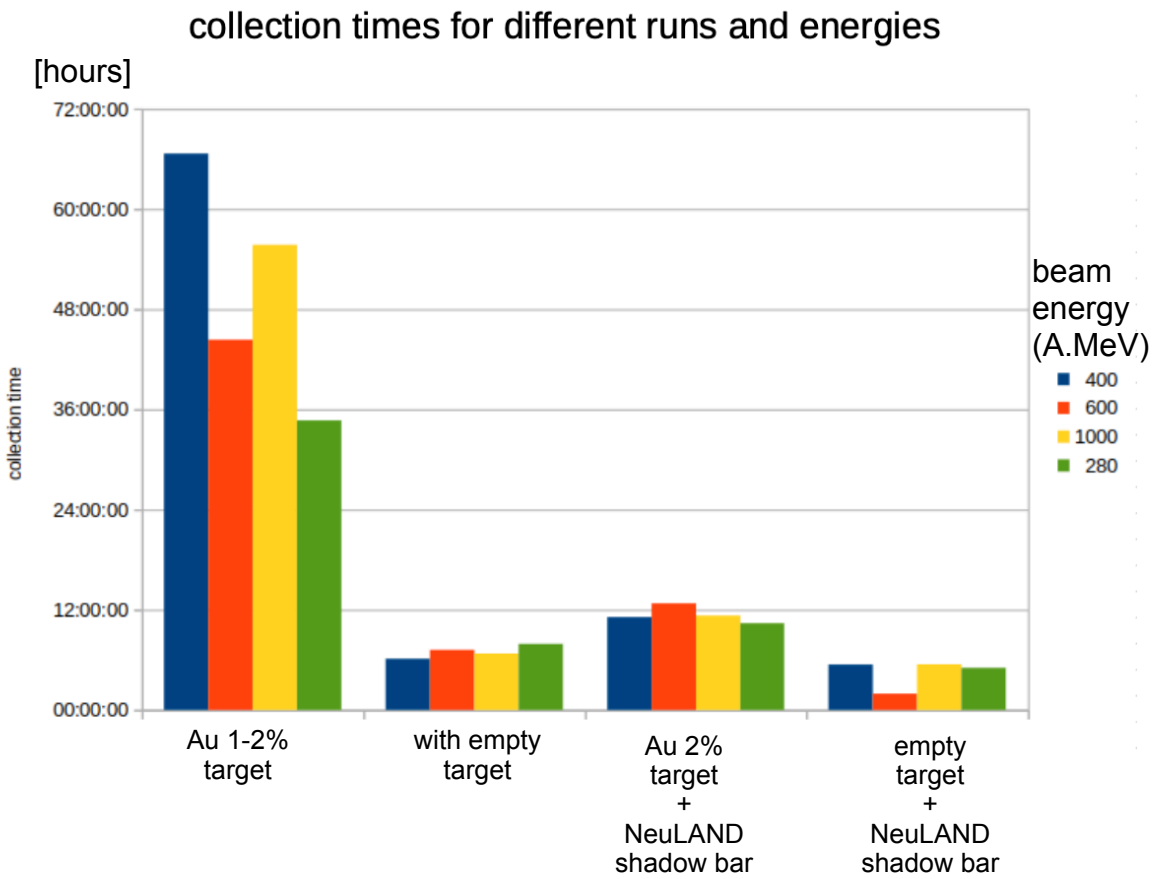

Reaction plane accuracy: CHIMERA - KRAB correlations

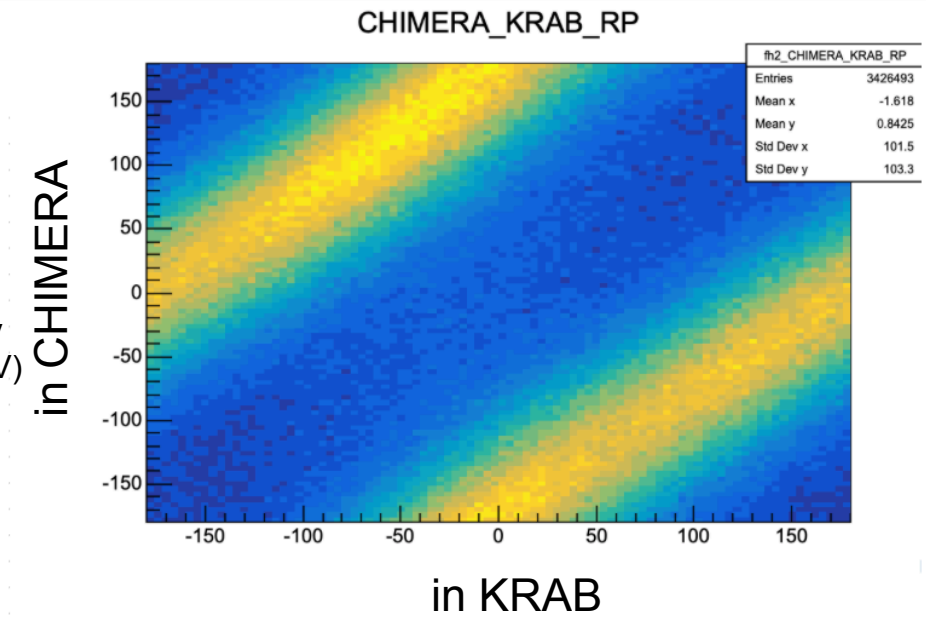

Reaction plane azimuthal angle (°) anti-correlation between KRAB and CHIMERA for **reactions in the target** (yellow bands); **else**: mostly reactions in air (blue background)
=> good signal/noise ratio.

Perspectives: Towards higher densities and precision

Symmetric nuclear matter EoS

- Constrained so far up to about $3\rho_0$ at GSI
- Above $3\rho_0$, AGS data have presumably constrained it up to around $3\text{-}7\rho_0$
- ... using the proton **directed flow** (F or v_1). But inconsistencies with experimental proton **elliptic flow** data comparing with FOPI data (up to 1.5A GeV)
- => **should be remeasured at FAIR** and **re-analysed with other transport models**.
- Above 1A GeV, elliptic flow still sensitive on K_0, up to around 3A GeV. **Directed flow is more constraining at higher incident energies.**

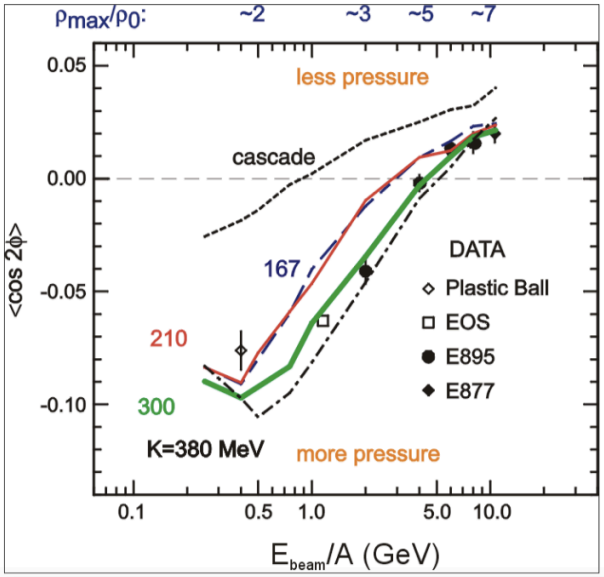

Pawel Danielewicz, *et al. Science* **298**, 1592 (2002); DOI: 10.1126/science.1078070

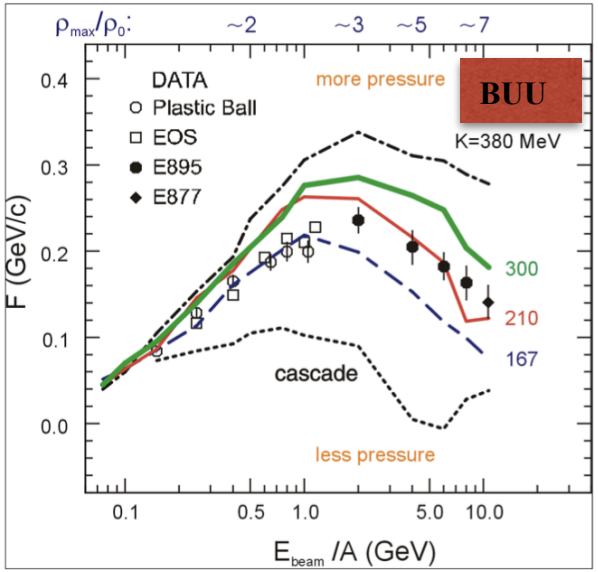

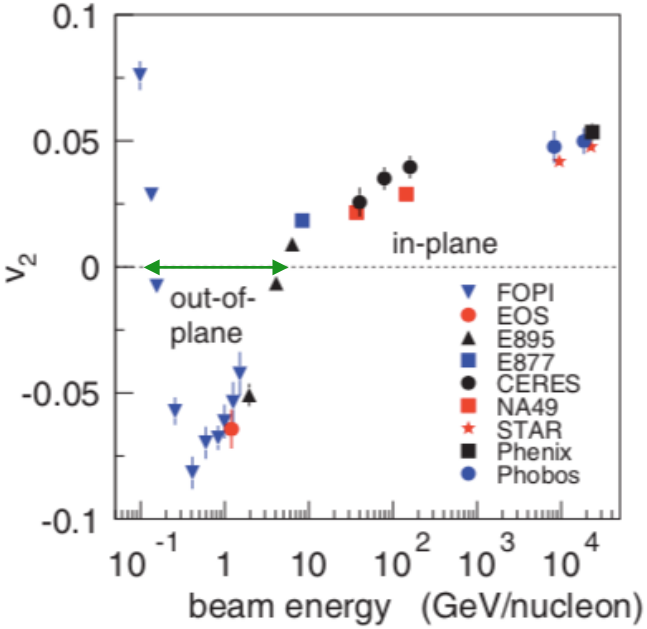

A. Le Fèvre *et al.*, Phys. Rev. C **98**, 034901 (2018)

Perspectives @FAIR (CBM, HADES, R3B)

Present situation: Above $\approx 2\rho_0$, the posterior distribution of the pressure in a neutron star is primarily driven by astronomical observations.
Reason: reliable HIC data (symmetry energy) not yet available at higher densities.

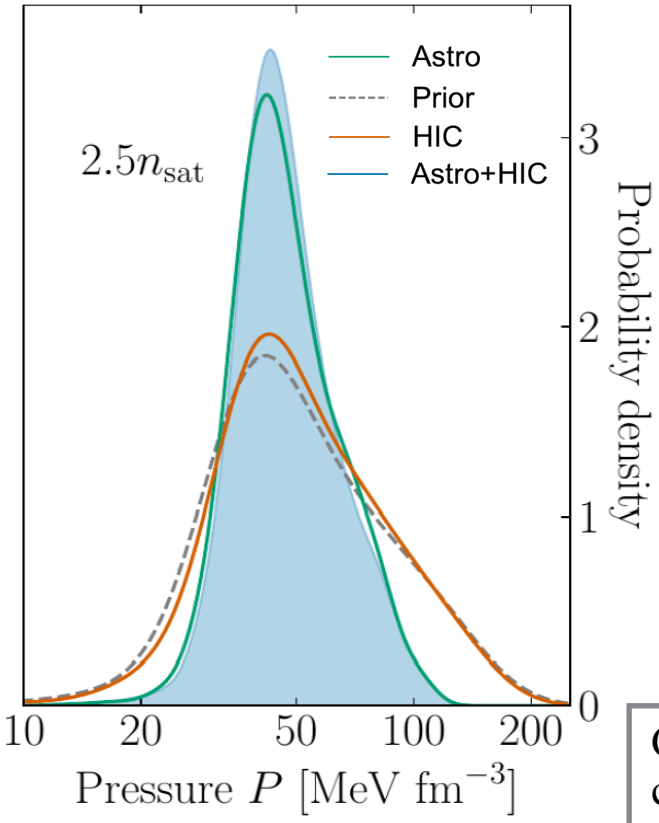

Challenge: which HIC observables will be able to constrain the symmetry energy at higher densities?
Cf. Dan Cozma's talk.

Perspectives @FAIR (CBM, HADES, R3B)

Present situation: Above $\approx 2\rho_0$, the posterior distribution of the pressure in a neutron star is primarily driven by astronomical observations.
Reason: reliable HIC data (symmetry energy) not yet available at higher densities.

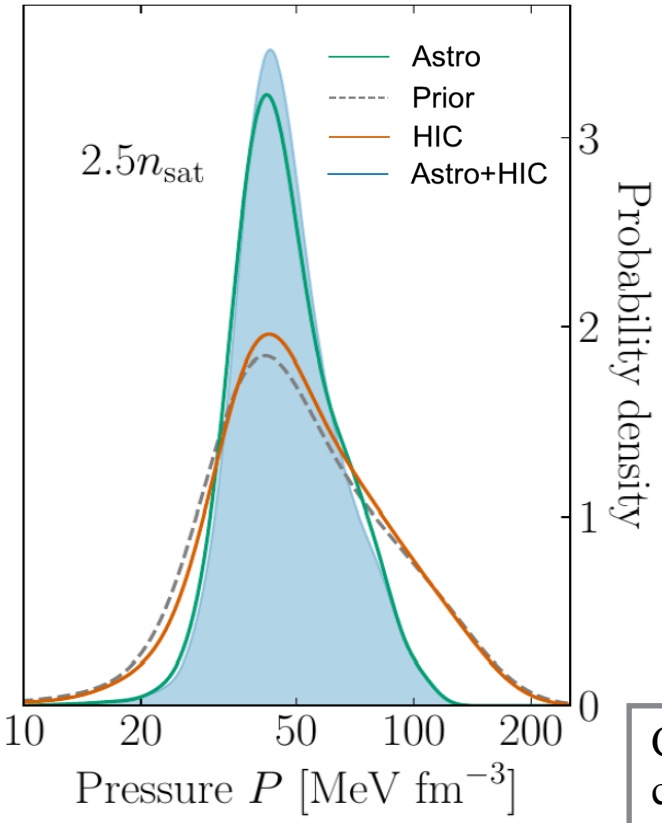

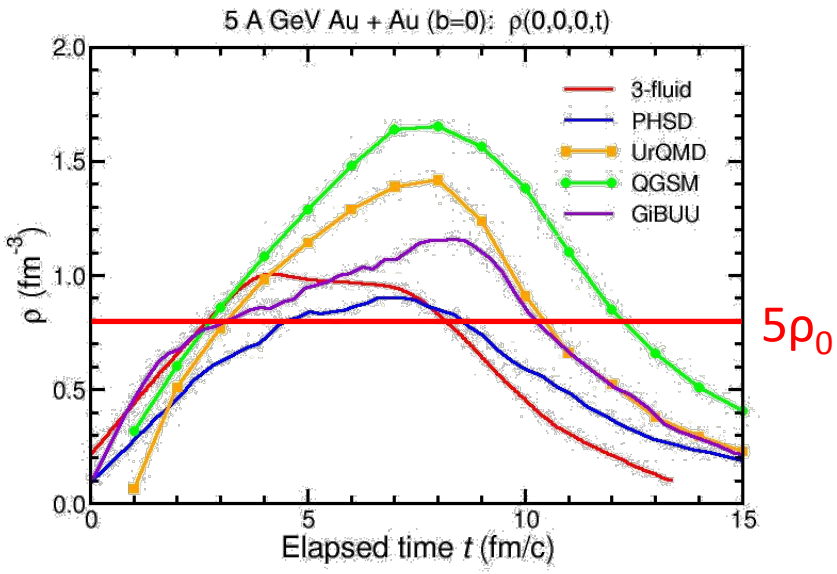

J. Randrup & J. Cleymans, PRC 74 (2006) 047901
I.C. Arsene et al., PRC 75 (2007) 034902
Friman et al., The CBM Physics Book, Springer (2010)

Challenge: which HIC observables will be able to constrain the symmetry energy at higher densities?
Cf. Dan Cozma's talk.

Perspectives: transport modelling improvements

A common HIC EoS with well-defined errors consistent with all transport codes

ELSEVIER

Progress in Particle and Nuclear Physics
Volume 134, January 2024, 104080

Review

Dense nuclear matter equation of state from heavy-ion collisions

Agnieszka Sorensen [1], Kshitij Agarwal [2], Kyle W. Brown [3 4], Zbigniew Chajęcki [5], Paweł Danielewicz [3 6], Christian Drischler [7], Stefano Gandolfi [8], Jeremy W. Holt [9 10], Matthias Kaminski [11], Che-Ming Ko [9 10], Rohit Kumar [3], Bao-An Li [12], William G. Lynch [3 6], Alan B. McIntosh [10], William G. Newton [12], Scott Pratt [3 6], Oleh Savchuk [3 13], Maria Stefaniak [14 15], Ingo Tews [8], ManYee Betty Tsang [3 6], Ramona Vogt [16 17], Hermann Wolter [18], Hanna Zbroszczyk [19], Navid Abbasi [20], Jörg Aichelin [21 22], Anton Andronic [23], Steffen A. Bass [24], Francesco Becattini [25 26], David Blaschke [27 28 29], Marcus Bleicher [30 31], Christoph Blume [32], Elena Bratkovskaya [15 30 31], B. Alex Brown [3 6], David A. Brown [33], Alberto Camaiani [25 26], Giovanni Casini [26], Katerina Chatziioannou [34 35], Abdelouahad Chbihi [36], Maria Colonna [37], Mircea Dan Cozma [38], Veronica Dexheimer [39], Xin Dong [40], Travis Dore [41], Lipei Du [42], José A. Dueñas [43], Hannah Elfner [15 30 22 31], Wojciech Florkowski [44], Yuki Fujimoto [1], Richard J. Furnstahl [14], Alexandra Gade [3 6], Tetyana Galatyuk [15 45], Charles Gale [42], Frank Geurts [46], Fabiana Gramegna [68], Sašo Grozdanov [47 48], Kris Hagel [10], Steven P. Harris [1], Wick Haxton [49 40], Ulrich Heinz [14], Michal P. Heller [50], Or Hen [51], Heiko Hergert [3 6], Norbert Herrmann [52], Huan Zhong Huang [53], Xu-Guang Huang [54 55 56], Natsumi Ikeno [57 10], Gabriele Inghirami [15], Jakub Jankowski [27], Jiangyong Jia [58 59], José C. Jiménez [60], Joseph Kapusta [61], Behruz Kardan [32], Iurii Karpenko [62], Declan Keane [39], Dmitri Kharzeev [63 59], Andrej Kugler [64], Arnaud Le Fèvre [15], Dean Lee [3 6], Hong Liu [65], Michael A. Lisa [14], William J. Llope [66], Ivano Lombardo [67], Manuel Lorenz [32], Tommaso Marchi [68], Larry McLerran [1], Ulrich Mosel [69 70], Anton Motornenko [22], Berndt Müller [24], Paolo Napolitani [71], Joseph B. Natowitz [10], Witold Nazarewicz [3 6], Jorge Noronha [72], Jacquelyn Noronha-Hostler [72], Grażyna Odyniec [40], Panagiota Papakonstantinou [73], Zuzana Paulínyová [74], Jorge Piekarewicz [75], Robert D. Pisarski [59], Christopher Plumberg [76], Madappa Prakash [7], Jørgen Randrup [40], Claudia Ratti [77], Peter Rau [1], Sanjay Reddy [1], Hans-Rudolf Schmidt [2 15], Paolo Russotto [37], Radoslaw Ryblewski [78], Andreas Schäfer [79], Björn Schenke [59], Srimoyee Sen [80], Peter Senger [81], Richard Seto [82], Chun Shen [66 83], Bradley Sherrill [3 6], Mayank Singh [61], Vladimir Skokov [84 83], Michał Spaliński [85 86], Jan Steinheimer [22], Mikhail Stephanov [87], Joachim Stroth [32 15], Christian Sturm [15], Kai-Jia Sun [88], Aihong Tang [59], Giorgio Torrieri [89 90], Wolfgang Trautmann [15], Giuseppe Verde [91], Volodymyr Vovchenko [77], Ryoichi Wada [10], Fuqiang Wang [92], Gang Wang [53], Klaus Werner [21], Nu Xu [40], Zhangbu Xu [59], Ho-Ung Yee [87], Sherry Yennello [10 9 93], Yi Yin [94]

Perspectives: transport mod

A common HIC EoS with well-defined errors consistent with all transport codes

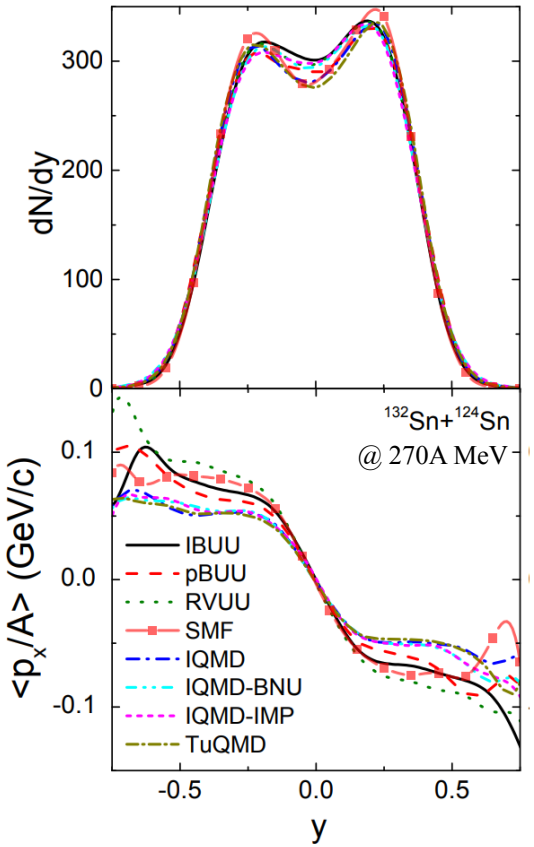

In line with the international Transport Model Evaluation Project (TMEP)

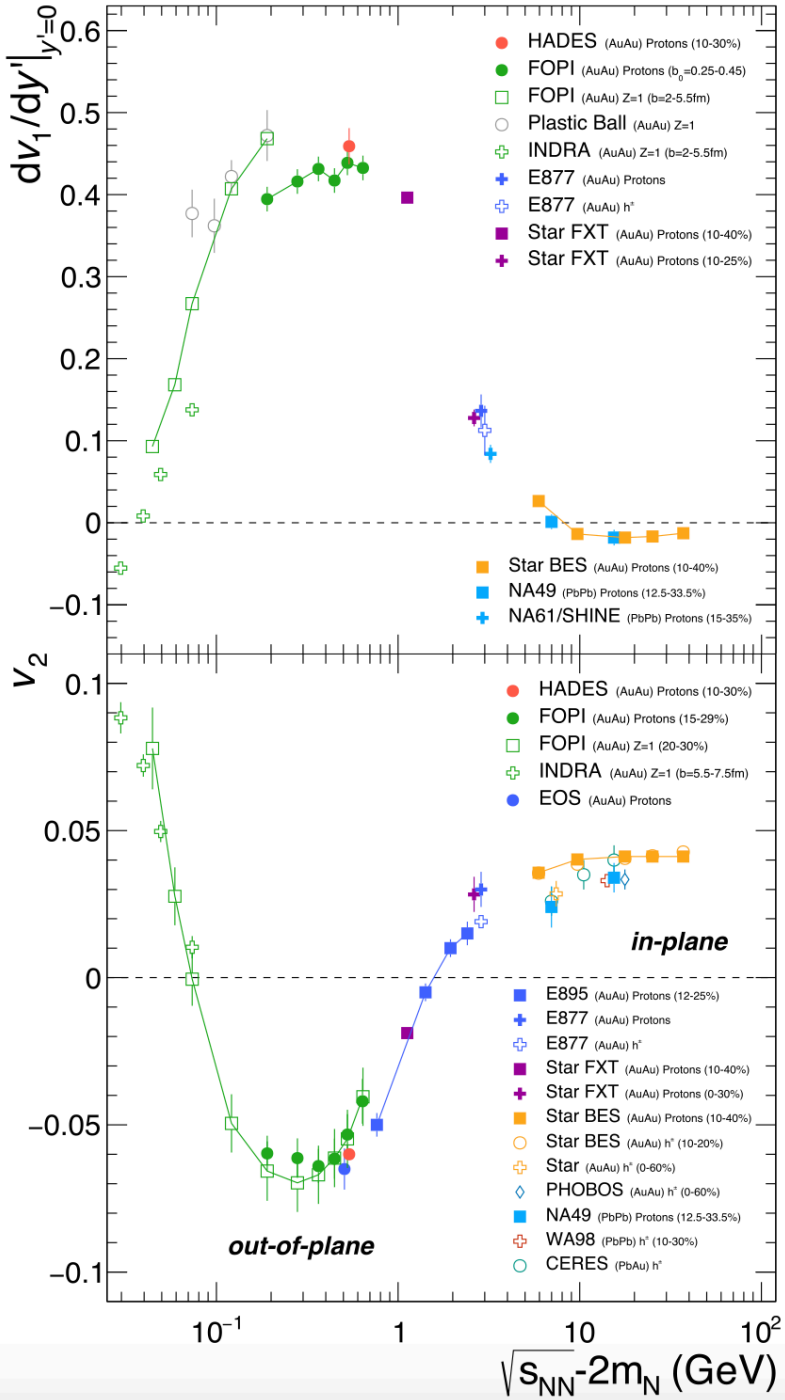

Perspectives: experimental programme

A promising multi-messenger era for the next 15+ years…

K. Agarwal

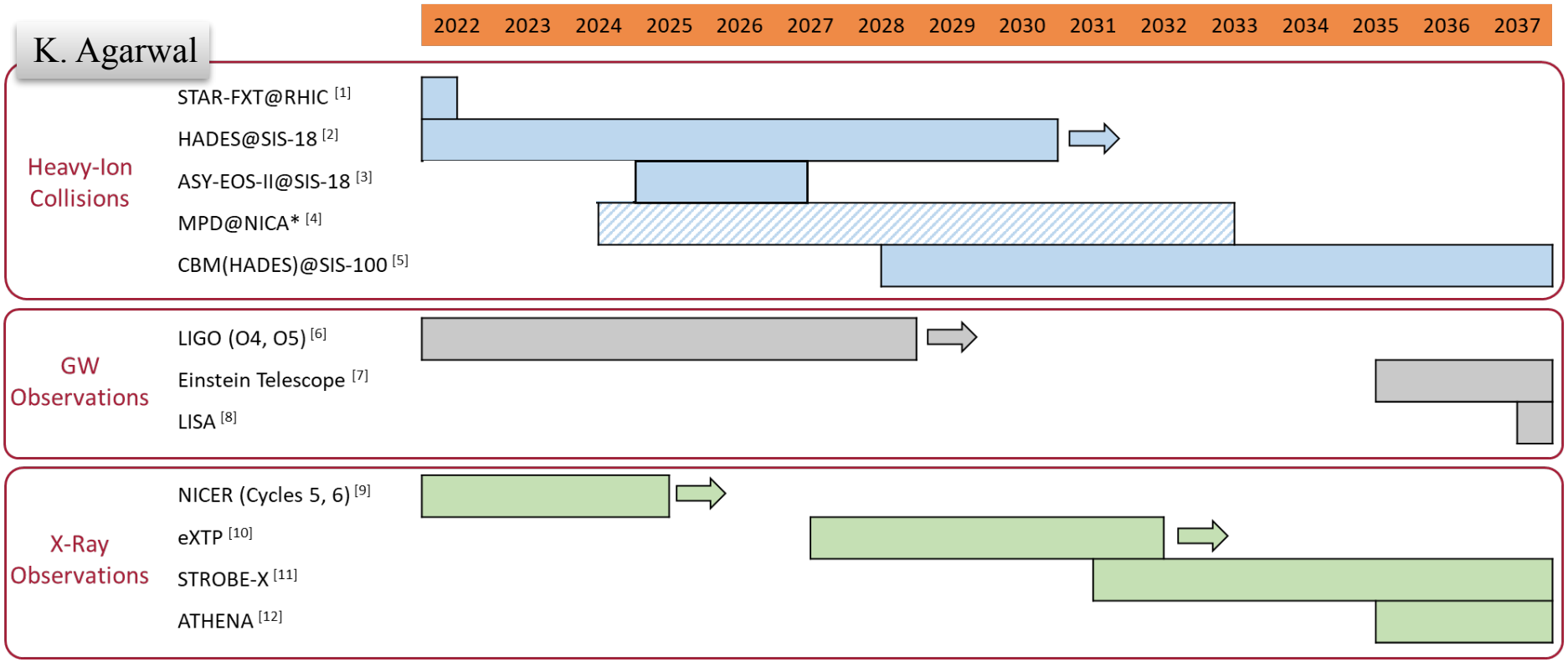

[1] D. Morrison, Quark Matter 2022 | Link
[2] Proposal for Beamtime in 2023-24, GSI G-PAC (2022)
[3] Proposal for Beamtime in 2023-24, GSI G-PAC (2022)
[4] I. Maldonado, A. Ayala, EuNPC 2022 | Link
[5] First-Science and Staging Review of the FAIR Project (2022) | Link
[6] LIGO-Virgo-KAGRA Observing Run Plan | Link
[7] Einstein Telescope Homepage | Link
[8] LISA ESA Factsheet | Link
[9] NICER Proposals Guide – Cycle 5 | Link
[10] eXTP Homepage | Link
[11] STROBE-X White Paper for the Astro 2020 Decadal Survey | Link
[12] ATHENA ESA Factsheet | Link

Conclusion and perspectives

Conclusion and perspectives

Conclusion and perspectives

Conclusion and perspectives

Conclusion and perspectives

Conclusion and perspectives

Conclusion and perspectives

Conclusion and perspectives

Conclusion and perspectives

Conclusion and perspectives

Conclusion and perspectives